

5-3-2008

## Development of a heterogeneously catalyzed chemical process to produce biodiesel

Alok Kumar Singh

Follow this and additional works at: <https://scholarsjunction.msstate.edu/td>

---

### Recommended Citation

Singh, Alok Kumar, "Development of a heterogeneously catalyzed chemical process to produce biodiesel" (2008). *Theses and Dissertations*. 1409.

<https://scholarsjunction.msstate.edu/td/1409>

This Dissertation - Open Access is brought to you for free and open access by the Theses and Dissertations at Scholars Junction. It has been accepted for inclusion in Theses and Dissertations by an authorized administrator of Scholars Junction. For more information, please contact [scholcomm@msstate.libanswers.com](mailto:scholcomm@msstate.libanswers.com).

DEVELOPMENT OF A HETEROGENEOUSLY CATALYZED CHEMICAL  
PROCESS TO PRODUCE BIODIESEL

By

Alok Kumar Singh

A Dissertation  
Submitted to the Faculty of  
Mississippi State University  
in Partial Fulfillment of the Requirements  
for the Degree of Doctor of Philosophy  
in Biological Engineering  
in the Department of Agricultural and Biological Engineering

Mississippi State, Mississippi

May 2008

DEVELOPMENT OF A HETEROGENEOUSLY CATALYZED CHEMICAL  
PROCESS TO PRODUCE BIODIESEL

By

Alok Kumar Singh

Approved:

---

Sandun D. Fernando  
Assistant Professor of Agricultural &  
Biological Engineering  
(Director of Dissertation and Graduate  
Coordinator)

---

S. D. Filip To  
Associate Professor of Agricultural &  
Biological Engineering  
(Committee Member)

---

Lester Pordesimo  
Assistant Professor of Agricultural &  
Biological Engineering  
(Committee Member)

---

Rafael Hernandez  
Assistant Professor of Chemical  
Engineering  
(Committee Member)

---

Juan L. Silva  
Professor of Food Science, Nutrition and  
Health Promotion  
(Committee Member)

---

W. Glenn Steele  
Interim Dean of the Bagley College of  
Engineering

Name: Alok Kumar Singh

Date of Degree: May 2, 2008

Institution: Mississippi State University

Major Field: Biological Engineering

Major Professor: Dr. Sandun D. Fernando

Title of Study: DEVELOPMENT OF A HETEROGENEOUSLY CATALYZED  
CHEMICAL PROCESS TO PRODUCE BIODIESEL

Pages in Study: 103

Candidate for Degree of Doctor of Philosophy

Biodiesel is a renewable, biodegradable, and nontoxic fuel. At present, when homogeneous catalysts are used, biodiesel is primarily produced in batch reactors in which the required energy is provided by heating accompanied by mechanical mixing. Alternatively, ultrasonic processing could be an effective way to attain required mixing while providing the necessary activation energy. We found that, using ultrasonication, a biodiesel yield in excess of 99% can be achieved in a short time duration of five minutes or less in comparison to one hour or more using conventional batch reactor systems. Homogeneous acid or base catalysts dissolve fully in the glycerol layer and partially in the fatty acid methyl esters (biodiesel) layer during the triglyceride transesterification process. Heterogeneous (solid) catalysts, on the other hand, can prevent catalyst contamination making product separation much easier. In the present work, one of the objectives was to determine the transesterification kinetics of different pure metal oxide catalysts, mixed metal oxide catalysts, layered double hydroxides with their corresponding yield is presented. It was found that heterogeneous catalysts require much

higher temperatures (215°C) and pressures to achieve acceptable conversion levels compared to homogeneous catalysts. For some of the mixed metal oxide solid catalysts a conversion level of 99% was observed. The present study also deals with the catalyst characterization on the basis of their acidity/ basicity and site strength, and surface area. Finally the deoxygenation of fatty acid methyl esters was carried out in order to upgrade the biodiesel. As a result, several aliphatic and aromatic hydrocarbons were detected in the mass spectrometric studies.

This dissertation consists of five chapters. Chapter I present a brief introduction, Chapter II contains a review of literature, Chapter III contains the materials and methods used in this study, Chapter IV presents the results and its discussions, Chapter V discusses the summary and conclusions and finally Chapter VI suggests some recommendations from the study.

Key words: heterogeneous catalysis, biodiesel, reaction kinetics, deoxygenation, thermodynamic analysis.

## DEDICATION

I would like to dedicate this research to my family members in India for their continuous support and encouragement throughout all stages of my life.

## ACKNOWLEDGEMENTS

I acknowledge my profound sense of gratitude and indebtedness to my research advisor Dr. Sandun D. Fernando, Assistant Professor, Department of Agricultural and Biological Engineering, Mississippi State University for his inspiring, helpful suggestions and persistent encouragements as well as close and consistent supervision through out the period of my Ph.D program. Being impeded by the limitations of earthly language skills, my expression of gratitude dares not come close to the justice so rightly deserved, however, I shall forever remain grateful for the lessons learned at the hand of such a gifted and revered mentor.

I would like to express my sincere gratitude to my committee members (alphabetically), Dr. Juan L. Siva, Dr. Lester Pordesimo, Dr. Rafael Hernandez and Dr. S. D. Filip To, for their suggestions in order to complete the research. My sincere thanks also go to all the faculty in the Department of Agricultural and Biological Engineering for their support.

I would like to extend my deep gratitude to all the bioenergy group members: Agus Haryanto, Dr. Shushil Adhikari, Saroj K. Jha, Dr. Shetian Liu, Dr. Xuejun Ye, Anuradh Gunawardena, and Gayan Nawaratna. I would also like to thank Ms. Sharron Miles, Kimberly Young, and Rhonda Walker Kinard for their help with paperwork and in numerous other ways.

I gratefully acknowledge the moral support and affection I received from my family members throughout my life. I also want to thank Sanju for her support and care during this endeavor. I guess a word of acknowledgement is not sufficient enough to express my indebtedness to all and sundry that unselfishly came forward to render unforgettable help during the project work.

Last but not the least, all thanks to the almighty for providing me this opportunity in my life.



## TABLE OF CONTENTS

|  | Page |
|--|------|
| DEDICATION .....                                       | ii   |
| ACKNOWLEDGEMENTS .....                                 | iii  |
| LIST OF TABLES .....                                   | viii |
| LIST OF FIGURES .....                                  | ix   |
| CHAPTER  |      |
| I. INTRODUCTION .....                                  | 1    |
| 1.1 Composition of Oils .....                          | 3    |
| 1.2 Composition of Biodiesel .....                     | 5    |
| 1.3 Mechanism of Transesterification .....             | 5    |
| 1.4 Justification of the Research .....                | 7    |
| 1.5 Objectives of the Study .....                      | 8    |
| II. REVIEW OF LITERATURE .....                         | 10   |
| 2.1 Use of Vegetable Oil as Diesel Fuel .....          | 10   |
| 2.2 Biodiesel Production using Ultrasonic Energy ..... | 15   |
| 2.3 Solid Catalysis in Biodiesel Production .....      | 17   |
| 2.4 Kinetics of Transesterification .....              | 20   |
| 2.5 Upgrading Biodiesel .....                          | 21   |
| III. MATERIALS AND METHODS .....                       | 24   |
| 3.1 Biodiesel Production Using Ultrasonication .....   | 24   |
| 3.1.1 Reagents and materials .....                     | 25   |
| 3.1.2 Equipment .....                                  | 25   |
| 3.1.3 Transesterification .....                        | 25   |
| 3.1.4 Gas chromatography analysis .....                | 26   |

|   |    |
|---|----|
| 3.2 Biodiesel Production with Solid Catalysts.....                                      | 27 |
| 3.2.1 Reagents and materials .....  | 27 |
| 3.2.2 Preparation of mixed metal oxides .....   | 27 |
| 3.2.3 Preparation of layered double hydroxides (LDH) .....                              | 28 |
| 3.2.4 Equipment .....   | 28 |
| 3.2.5 Transesterification of soybean oil.....   | 28 |
| 3.2.6 Transesterification for kinetics analysis.....                                    | 29 |
| 3.2.7 Gas chromatography analysis .....   | 30 |
| 3.3 Catalyst Characterization.....  | 30 |
| 3.3.1 Determination of surface area of the catalysts.....                               | 30 |
| 3.3.2 Determination of acid/base strength .....   | 30 |
| 3.3.3 Determination of acidity /basicity.....   | 31 |
| 3.3.4 X- ray Diffractogram and Scanning Electron Microscope analysis .....              | 32 |
| 3.4 Kinetics of Transesterification.....  | 32 |
| 3.5 Biodiesel Upgrading .....   | 35 |
| 3.5.1 Thermodynamic analysis .....  | 36 |
| 3.5.2 Materials and methods used in deoxygenation of Biodiesel.....                     | 38 |
| <br>  |    |
| IV. RESULTS AND DISCUSSION.....   | 40 |
| <br>  |    |
| 4.1 Ultrasonic Processing for Biodiesel Production .....                                | 40 |
| 4.1.1 Effect of amplitude .....   | 42 |
| 4.1.2 Effect of input energy .....  | 44 |
| 4.2 Biodiesel Production with Solid Catalysts.....                                      | 45 |
| 4.2.1 Transesterification with metal oxides .....                                       | 45 |
| 4.2.2 Screening of mixed metal oxides.....  | 48 |
| 4.2.3 Screening of layered double hydroxides.....                                       | 51 |
| 4.3 Catalyst Characterization.....  | 53 |
| 4.3.1 Surface area of the catalysts.....  | 53 |
| 4.3.2 Acidity/ Basicity of the catalysts .....  | 54 |
| 4.3.3 Leaching analysis.....  | 56 |
| 4.3.4 X-Ray Diffractogram (XRD) and Scanning Electron Microscope<br>(SEM) analysis..... | 57 |
| 4.4 Reaction Kinetics Determination.....  | 62 |
| 4.5 Reactor Modeling.....   | 64 |
| 4.6 Biodiesel Upgrading .....   | 67 |
| 4.6.1 Mass spectrometer results .....   | 67 |
| 4.6.2 Thermodynamic analysis of methyl linoleate.....                                   | 75 |
| <br>  |    |
| V. SUMMARY AND CONCLUSIONS .....  | 83 |
| <br>  |    |
| 5.1 Summary.....  | 83 |
| 5.2 Conclusions.....  | 85 |

|                          |    |
|--------------------------|----|
| VI. RECOMMENDATIONS..... | 86 |
| LITERATURES CITED.....   | 88 |
| APPENDIX                 |    |
| A.....                   | 94 |
| B.....                   | 97 |

## LIST OF TABLES

| TABLE  | Page |
|--|------|
| 1.1 Chemical properties of vegetable oil on the basis of their fatty acid composition, % by weight (Ma, 1999) .....      | 4    |
| 1.2 Typical fatty acid composition-common oil source (Ma, 1999).....   | 4    |
| 1.3 Chemical structures of common fatty acid and their methyl esters .....   | 5    |
| 4.1 Effects of amplitude, reaction time on yield of biodiesel via ultrasonication .....                                  | 43   |
| 4.2 Surface area of the metal oxides .....   | 54   |
| 4.3 Site strength of the metal oxides and their respective acidity/basicity value .....                                  | 55   |
| 4.4 Leaching of metals from their respective metal oxide in biodiesel and glycerol sample .....                          | 57   |
| 4.5 Elemental analysis of NaMO1, NaMO2, NaMO3 and NaMO4 .....  | 59   |
| 4.6 The value of coefficient of correlation ( $R^2$ ) of all eight cases for each catalyst....                           | 63   |
| 4.7 Reaction order of the transesterification w.r.t. each of the reactant as well as overall and the rate constant ..... | 64   |
| 4.8 Values of activation energy and pre-exponential factor for NaMO1 .....   | 67   |
| 4.9 Number of moles of different hydrocarbons deoxygenated from one mole of methyl linoleate at 375 °C.....              | 82   |

## LIST OF FIGURES

| FIGURE   | Page |
|--|------|
| 1.1 Transesterification of triglyceride to mixture of alkyl esters (Biodiesel).....  | 3    |
| 4.1 Biodiesel yield variations with time and sonic wave amplitude.....   | 41   |
| 4.2 Input energy variations with time and sonic wave amplitude.....  | 41   |
| 4.3 Temperature variations with time and sonic wave amplitude .....  | 42   |
| 4.4 Effect of input energy on the fatty acid methyl esters yield .....   | 44   |
| 4.5 FAME yield with different solid catalysts .....  | 45   |
| 4.6 FAME yield for PbO, MgO, MnO <sub>2</sub> , BaO and CaO (reaction times denoted<br>represent time after reactants reached 215°C) ..... | 47   |
| 4.7 FAME yield for BaO and CaO (reaction times denoted represent time after<br>reactants reached 215°C).....                               | 48   |
| 4.8 FAME yield for NaMO1 at two different temperatures .....   | 49   |
| 4.9 FAME yield for NaMO2 at two different temperatures .....   | 49   |
| 4.10 FAME yield for NaMO3 at two different temperatures .....  | 50   |
| 4.11 FAME yield for NaMO4 at two different temperatures .....  | 50   |
| 4.12 FAME yield with LiLDH at 15:1 methanol to oil ratio and 1 % (by wt.) of the<br>catalyst for 1 hr of transesterification .....         | 51   |
| 4.13 FAME yield with LiLDH at 40:1 methanol to oil ratio and 1 % (by wt.) of the<br>catalyst for 2 hr of transesterification .....         | 52   |
| 4.14 FAME yield with LiLDH at 15:1 methanol to oil ratio and 3 % (by wt.) of the<br>catalyst for 4 hr of transesterification .....         | 53   |

|  |    |
|--|----|
| 4.15 SEM images of (a)- NaMO1, (b)- NaMO2, (c)- NaMO3 and (d)- NaMO4.....  | 58 |
| 4.16 X-ray patterns for NaMO1 .....  | 60 |
| 4.17 X-ray patterns for NaMO2.....   | 61 |
| 4.18 X-ray patterns for NaMO3.....   | 61 |
| 4.19 X-ray patterns for NaMO4.....   | 62 |
| 4.20 Conversion of Linoleic acid to methyl linoleate at 115°C and 1:6 oil to methanol<br>ratio w.r.t. time with NaMO1..... | 69 |
| 4.21 Conversion of Linoleic acid to methyl linoleate at 215°C and 1:6 oil to methanol<br>ratio w.r.t. time with NaMO1..... | 70 |
| 4.22 Conversion of Linoleic acid to methyl linoleate at 315°C and 1:6 oil to methanol<br>ratio w.r.t. time with NaMO1..... | 71 |
| 4.23 Conversion of Linoleic acid to methyl linoleate at 215°C and 1:3 oil to methanol<br>ratio w.r.t. time with NaMO1..... | 72 |
| 4.24 Conversion of Linoleic acid to methyl linoleate at 215°C and 1:6 oil to methanol<br>ratio w.r.t. time with NaMO1..... | 73 |
| 4.25 Conversion of Linoleic acid to methyl linoleate at 215°C and 1:9 oil to methanol<br>ratio w.r.t. time with NaMO1..... | 74 |
| 4.26 Comparison of experimental and the model reaction rate at 215°C w.r.t. time<br>using rate model with NaMO1.....       | 75 |
| 4.27 Spectrum of deoxygenation of biodiesel with HZSM-5 at 215 °C .....  | 76 |
| 4.28 Spectrum of deoxygenation of biodiesel with HZSM-5 at 315 °C .....  | 77 |
| 4.29 Spectrum of deoxygenation of biodiesel with HZSM-5 at 375 °C .....  | 78 |
| 4.30 Detected peaks of deoxygenated compounds on the mass spectrometer.....  | 79 |
| 4.31 Thermodynamic analysis of Methyl Linoleate.....   | 81 |

## CHAPTER I

### INTRODUCTION

The status of present consumption of crude oil is about 79 millions barrels per day. The tremendous increasing need of oil, which is predicted to be about 119 millions barrels per day by 2020's and the shortage of oil thereafter (after 10-15 years), predicted based on the total reserves in hand, urgently urges to focus the research in finding alternative means to fulfill world's energy needs. The development of energy efficient biofuel production technologies in aiming at reducing the reagent costs and increasing the production efficiency is becoming important in a world that is increasingly becoming "green". In this prospect, extraction of fuel energy in the form of fatty acid methyl or ethyl esters, commonly known as biodiesel, from vegetable oils and animal fats is becoming more popular due to its renewable nature, ability to replace dwindling petroleum based production technologies, for being environmental friendly, and overwhelming opportunities to overcome an imminent forthcoming energy crisis. Biodiesel is generally defined as the monoalkyl esters made from triglycerides, diglycerides and mono-glycerides. The triglycerides could originate from vegetable oils or animal fats. This renewable fuel is as effective as petroleum diesel in powering unmodified or slightly modified diesel engines. It is biodegradable and nontoxic, has low undesirable tailpipe emission profiles, and, therefore, is environmentally benign.

There are different methods of biodiesel production and application such as direct use and blending, microemulsions, thermal cracking (Pyrolysis) of vegetable oil and transesterification (Ma 1999). Among these, the most common method of biodiesel production is transesterification (alcoholysis) of oil (triglycerides) with methanol in the presence of a catalyst which gives biodiesel (fatty acid methyl esters) and glycerol (byproduct). The selection of catalyst depends on the amount of FFA present in the oil. Generally, the catalysts are alkali, acid, or enzyme. For triglyceride stock having lower amount of FFAs, alkali catalyzed reaction gives a better conversion in a relatively short time while for higher FFAs containing stock, acid catalyzed esterification followed by transesterification is suitable (Schuchardt 1998). The stoichiometric reaction requires 1 mole of triglyceride and 3 moles of alcohol. However, excess alcohol is used to drive the reversible reaction forward to increase the yields of the alkyl esters and to assist phase separation from the glycerol formed. Several aspects, including the type of catalyst (alkaline or acid), alcohol/vegetable oil molar ratio, temperature, purity of the reactants (mainly water content), and free fatty acid content, have an influence on the transesterification rates (Schuchardt 1998). Figure 1.1 shows the reaction of soybean oil (triglyceride) with alcohol in the presence of a catalyst producing biodiesel (mixture of alkyl esters) and glycerol (Schuchardt 1998). Alkali-catalyzed transesterification is much faster than acid-catalyzed transesterification and is the most commonly used method commercially (Ma 1999). Putting that together with the fact that the alkaline catalysts are less corrosive than acidic compounds, industrial processes usually favor base catalysts such as alkaline metal alkoxides and hydroxides as well as sodium or potassium



carbonates.

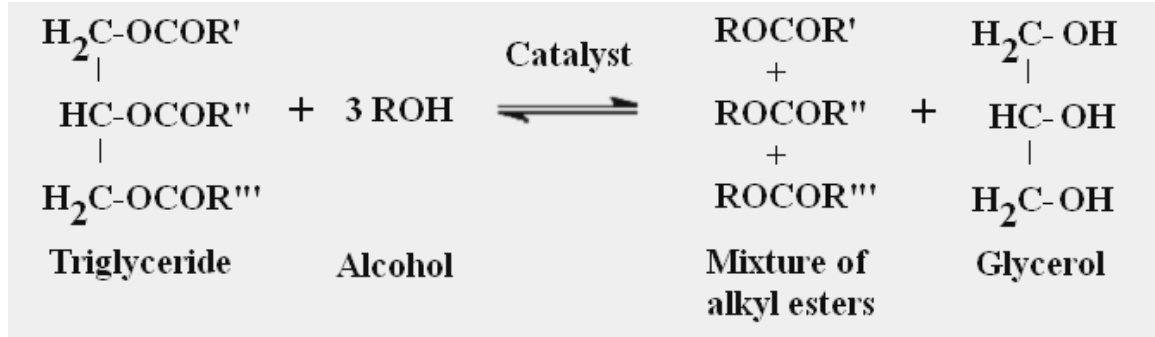


Figure 1.1 Transesterification of triglyceride to mixture of alkyl esters (Biodiesel)

### 1.1 Composition of Oils

Fats and oils are primarily water-insoluble hydrophobic substances of plant and animal origin and are made up of one mole of glycerol and three moles of fatty acids and are commonly referred to as triglycerides. Fatty acids vary in carbon chain length and in the number of unsaturated bonds (double bonds). The fatty acids found in vegetable oils are summarized in Table 1.1. Table 1.2 shows typical fatty acid compositions of common oil sources. Natural vegetable oils and animal fats are solvent extracted or mechanically pressed to obtain crude oil or fat. These usually contain free fatty acids, phospholipids, sterols, water, odorants and other impurities. Even refined oils and fats contain small amounts of free fatty acids and water. The free fatty acid and water contents have significant effects on the transesterification of glycerides with alcohols using alkaline or acid catalysts. They also interfere with the separation of fatty acid alkyl esters and glycerol because of salt formation in the product.

Table 1.1 Chemical properties of vegetable oil on the basis of their fatty acid composition, % by weight (Ma, 1999)

| <b>Vegetable Oil</b> | <b>16:0</b> | <b>18:0</b> | <b>20:0</b> | <b>22:0</b> | <b>24:0</b> | <b>18:1</b> | <b>22:1</b> | <b>18:2</b> | <b>18:3</b> |
|----------------------|-------------|-------------|-------------|-------------|-------------|-------------|-------------|-------------|-------------|
| Corn                 | 11.67       | 1.85        | 0.24        | 0.00        | 0.00        | 25.16       | 0.00        | 60.60       | 0.48        |
| Cottonseed           | 28.33       | 0.89        | 0.00        | 0.00        | 0.00        | 13.27       | 0.00        | 57.51       | 0.00        |
| Cramble              | 2.07        | 0.70        | 2.09        | 0.80        | 1.12        | 18.86       | 58.51       | 9.00        | 6.85        |
| Peanut               | 11.38       | 2.39        | 1.32        | 2.52        | 1.23        | 48.28       | 0.00        | 31.95       | 0.93        |
| Rapeseed             | 3.49        | 0.85        | 0.00        | 0.00        | 0.00        | 64.40       | 0.00        | 22.30       | 8.23        |
| Soybean              | 11.75       | 3.15        | 0.00        | 0.00        | 0.00        | 23.26       | 0.00        | 55.53       | 6.31        |
| Sunflower            | 6.08        | 3.26        | 0.00        | 0.00        | 0.00        | 16.93       | 0.00        | 73.73       | 0.00        |

Table 1.2 Typical fatty acid composition-common oil source (Ma, 1999)

| <b>Fatty acid</b> | <b>Soybean</b> | <b>Cottonseed</b> | <b>Palm</b> | <b>Lard</b> | <b>Tallow</b> | <b>Coconut</b> |
|-------------------|----------------|-------------------|-------------|-------------|---------------|----------------|
| Lauric            | 0.1            | 0.1               | 0.1         | 0.1         | 0.1           | 46.5           |
| Myristic          | 0.1            | 0.7               | 1.0         | 1.4         | .8            | 19.2           |
| Palmitic          | 0.2            | 20.1              | 42.8        | 23.6        | 23.3          | 9.8            |
| Stearic           | 3.7            | 2.6               | 4.5         | 14.2        | 19.4          | 3.0            |
| Oleic             | 22.8           | 19.2              | 40.5        | 44.2        | 42.4          | 6.9            |
| Linoleic          | 53.7           | 55.2              | 10.1        | 10.7        | 2.9           | 2.2            |
| Linolenic         | 8.6            | 0.6               | 0.2         | 0.4         | 0.9           | 0.0            |

## 1.2 Composition of Biodiesel

Biodiesel is mixture of fatty acid alkyl esters. If methanol is used as a reactant, it will be a mixture of fatty acid methyl esters (FAME). Based on the feed stock, biodiesel has different proportions of fatty acid methyl esters. Table 1.3 shows the chemical composition of common fatty acids and their methyl esters present in the biodiesel.

Table 1.3 Chemical structures of common fatty acid and their methyl esters.

| <b>Fatty acid /<br/>Formula/<br/>Molecular weight</b> | <b>Common<br/>acronym</b> | <b>Methyl ester/<br/>Formula/<br/>Molecular weight</b> |
|---|---------------------------|--|
| Palmitic acid/<br>$C_{16}H_{32}O_2$ /<br>256.428      | C16:0                     | Methyl Palmitate/<br>$C_{17}H_{34}O_2$ /<br>270.457    |
| Stearic acid/<br>$C_{18}H_{36}O_2$ /<br>284.481       | C18:0                     | Methyl Stearate/<br>$C_{19}H_{38}O_2$ /<br>298.511     |
| Oleic acid/<br>$C_{18}H_{34}O_2$ /<br>282.465         | C18:1                     | Methyl Oleate/<br>$C_{19}H_{36}O_2$ /<br>296.495       |
| Linoleic acid/<br>$C_{18}H_{32}O_2$ /<br>280.450      | C18:2                     | Methyl Linoleate/<br>$C_{19}H_{34}O_2$ /<br>294.479    |
| Linolenic acid/<br>$C_{18}H_{30}O_2$ /<br>278.434     | C18:3                     | Methyl Linolenate/<br>$C_{19}H_{32}O_2$ /<br>292.463   |

## 1.3 Mechanism of Transesterification

As mentioned earlier, the selection of a catalyst depends on the amount of free fatty acids (FFA) content of the triglyceride feedstock. For our analysis we used soybean oil for all the transesterification experiments which had a FFA content of less than 1 %. Therefore, we used base as the catalyst in all of our preliminary (and control) transesterification reactions. Equation 1.1 to 1.4 shows the mechanism of base catalyzed transesterification.



#### **1.4 Justification of the Research**

Conventionally homogeneous catalysts (like NaOH, KOH etc.) are used for the transesterification reaction. Since the transesterification reaction can only occur in the interfacial region between the liquids (Benitez, 2004) and also fats and alcohols are not totally miscible (Stavarache, 2003, 2005), this is a very slow process. A vigorous mixing is required to increase the area of contact between the two immiscible phases, and thus produce an emulsion. In the base-catalyzed procedure, some soap is formed and it acts as a phase transfer catalyst, thus helping the mixing of the reactants (Stavarache, 2005). Ultrasonication provides the mechanical energy for mixing and the required energy for initiating the transesterification reaction (Benitez, 2004). Low frequency ultrasonic irradiation is a useful tool for emulsification of immiscible liquids. The collapse of the cavitation bubbles disrupts the phase boundary and causes emulsification by ultrasonic jets that impinge one liquid to another.

Despite industrial applicability, homogeneous catalysts have their own limitations, especially those associated with homogeneously catalyzed processes. The catalyst dissolves fully in the glycerin layer and partially in the FAME layer. As a result, biodiesel should be cleaned through a slow, tedious and an environmentally unfriendly water washing process. Catalyst contaminated glycerin has little value in today's market and is increasingly becoming a disposal issue. Another negative aspect of the homogeneously catalyzed process is that the catalysts are not re-usable. Heterogeneous catalysts, on the other hand, make product separation easier and make catalysts reusable. With the use of solid catalysts, the refining steps in the purification process can be

reduced. Also, heterogeneous catalysts have the potential to simplify the production process by enabling usage of continuous packed bed reactors.

In most of the solid catalyzed experiments, the reaction proceeded at a relatively slow rate (Gryglewicz, 1999). The presence of heterogeneous catalysts makes the reaction mixture a three-phase system, oil-methanol-catalyst (L/L/S - corresponding to a hydrophobic liquid phase, hydrophilic liquid phase and a solid catalyst phase), which for mass transfer reasons, protracts the reaction. At the same time, heterogeneous catalysis requires relatively harsher reaction conditions, i.e., high pressures and high temperatures. For example, some experiments have been carried out at temperatures as low as 78 K and as high as 1000 K and high pressures, with high pressure and temperature favoring better conversion (Li, 2005).

This research was undertaken keeping the above mentioned problem in mind.

### **1.5 Objectives of the Study**

Based on the intricacies associated with the homogeneously catalyzed transesterification process, the overall goal of this study is to design and develop a heterogeneously catalyzed chemical process to produce biodiesel in an efficient manner.

The specific objectives are as follows:

1. Evaluate the feasibility of using ultrasonication (ultrasound energy) for fast mixing of transesterification reactant to produce the biodiesel.
2. Identify a functional heterogeneous (solid) catalyst for the transesterification via catalyst screening -Metal Oxides, Mixed Oxides and Layered Double Hydroxides (LDH).

3. Study the catalytic properties of active heterogeneous catalysts via catalyst surface characterization and chemical kinetics determination.
4. Identify a process to upgrade biodiesel via deoxygenation of fatty acid methyl esters (biodiesel).

## CHAPTER II

### REVIEW OF LITERATURE

This chapter contains the literature cited in this study. Section 2.1 presents a brief history of the use of vegetable oil as a diesel fuel. Section 2.2 contains the history of biodiesel production using ultrasonication, followed by the background of solid catalysis in biodiesel production in section 2.3. Section 2.4 depicts background of reaction kinetics determination on solid catalysis work. Finally section 2.5 will represent the history of upgrading biodiesel.

#### **2.1 Use of Vegetable Oil as Diesel Fuel**

Vegetable oils have long been promoted as possible substitutes for diesel fuel. Gauthier, a French engineer, published a paper in 1928 discussing the use of vegetable oils in diesel engines. Interest in vegetable oils continued in various parts of the world during the Second World War, but later on, the arrival of peace and the relative abundance of inexpensive fossil fuels made research into diesel substitutes unnecessary. Castor oil was used in the first diesel engine in Argentina in 1916 (De Vedia, 1944). Historical records indicate that Rudolph Diesel, the inventor of the diesel engine, used vegetable oil in his engine as early as 1900 (Peterson, 1986). Castor oil was used in the first diesel engine in Argentina in 1916 (De Vedia, 1944).



However, owing to oil embargoes in the late 1970's and worldwide interest on environmentally friendly energy alternatives, there was a renewed vigor on alternative fuels research and as a result considerable work has recently been done on vegetable oils as an alternative to diesel fuel. That research included palm oil, soybean oil, sunflower oil, coconut oil, rapeseed oil and tung oil (Ma, 1999). Animal fats, although mentioned frequently, have not been studied to the same extent as vegetable oils. Some processing methods applicable to vegetable oils are not applicable to animal fats because of natural physical property differences. Oils from algae, bacteria and fungi also have been investigated. (Shay, 1993). Microalgae have been examined as a source of methyl esters diesel fuel (Nagel, 1990). Terpenes and latexes also were studied as diesel fuels (Calvin, 1985).

After the energy crisis in the 1980's, there has been considerable interest in using vegetable oils as a fuel. Bartholomew (1981) addressed the concept of using food (with oil content) for fuel, indicating that petroleum should be the "alternative" fuel rather than vegetable oil and alcohol. He also argued that some form of renewable energy other than alternatives from food sources should take the place of the nonrenewable resources.

The most advanced work with sunflower oil occurred in South Africa because of the oil embargo. Caterpillar Brazil, in 1980 (Bartholomew, 1981), used pre-combustion chamber engines with a mixture of 10% vegetable oil to maintain total power without any alterations or adjustments to the engine. They soon found out that it was not practical to substitute 100% vegetable oil for diesel fuel. However, a blend of 20% vegetable oil and 80% diesel fuel was found to be successful. Some short-term experiments used up to a 50/50 ratio with varying success rates. The first international Conference on Plant and

Vegetable Oils as fuels was held in Fargo, North Dakota in August 1982. The primary concerns discussed were the cost of the fuel, effects of vegetable oil fuels on engine performance and durability and fuel preparation, specifications, and effects of additives. Oil production, oilseed processing and extraction also were considered in this meeting (ASAE, 1982). Some ground work on use of neat triglycerides in compression ignition engines was promulgated at this meeting.

In one such study, a diesel fleet was powered with filtered, used frying oil (Anon, 1982). Neat (100%) used cooking oil and a blend of 95% used cooking oil and 5% diesel fuels were used. Blending or preheating was used as needed to compensate for cooler ambient temperatures. It was reported that there were no coking and carbon build-up problems. The key was suggested to be filtering and the only problem reported was lubricating oil contamination (viscosity increase due to polymerization of polyunsaturated vegetable oils). The lubricating oil had to be changed every 6,400 – 7,200 km. The advantages of vegetable oils as diesel fuel are (1) liquid nature-portability, (2) heat content (80% of diesel fuel), (3) readily availability and (4) renewability. The disadvantages are (1) higher viscosity, (2) lower volatility and (3) the reactivity of unsaturated hydrocarbon chains (Pryde, 1983).

Problems related to using direct triglycerides appeared to emerge only after the engine has been operated for longer periods of time, especially with direct-injection engines. The problems include (1) coking and trumpet formation on the injectors to such an extent that fuel atomization does not occur properly or is even prevented as a result of plugged orifices, (2) carbon deposits, (3) oil ring sticking and (4) thickening and gelling of the lubricating oil as a result of contamination by the vegetable oils. Mixtures of

degummed soybean oil and No. 2 diesel fuel in the ratios of 1:2 and 1:1 were tested for engine performance and crankcase lubricant viscosity in a John Deere 6-cylinder, 6.6 L displacement, direct-injection, turbocharged engine for a total of 600 h (Adams et al., 1983). The lubricating oil thickening and potential gelling existed with the 1:1 blend, but it did not occur with the 1:2 blend. The results indicated that 1:2 blend should be suitable as a fuel for agricultural equipment during periods of diesel fuel shortages or allocations.

Schlick et al. (1988) evaluated the performance of a direct injection 2.59 L, 3-cylinder 2600 series Ford diesel engine operating on mechanically expelled-unrefined soybean oil and sunflower oil blended with number 2 diesel fuels on a 25:75 v/v basis. The power remained constant throughout 200 h of operation. Excessive carbon deposits on all combustion chamber parts precluded the use of these fuel blends, at least for the particular test engine under the specified operating conditions. Ziejewski et al. (1984) prepared an emulsion of 53% (vol) alkali-refined and winterized sunflower oil, 13.3% (vol) 190-proof ethanol and 33.4% (vol) 1-butanol. This nonionic emulsion had a viscosity of 6.31 cSt at 40°C, a cetane number of 25 and an ash content of less than 0.01%. Lower viscosities and better spray patterns (more even) were observed with an increase of 1-butanol. In a 200 h laboratory screening endurance test, no significant deteriorations in performance were observed, but irregular injector needle sticking, heavy carbon deposits, incomplete combustion and an increase of lubricating oil viscosity were reported. Schwab et al. (1987) used the ternary phase equilibrium diagram and the plot of viscosity versus solvent fraction to determine the emulsified fuel formulations. All microemulsions with butanol, hexanol and octanol met the maximum viscosity requirement for No. 2 diesel. The 2-octanol was an effective amphiphile in the micellar

solubilization of methanol in triolein and soybean oil. Methanol was often used due to its economic advantage over ethanol.

The first pyrolysis of vegetable oil was conducted in an attempt to synthesize petroleum from vegetable oil (Chang and Wan, 1947). Since World War I, many investigators have studied the pyrolysis of vegetable oils to obtain products suitable for fuel. In 1947, a large scale study on thermal cracking of tung oil using calcium soaps was reported (Chang and Wan, 1947). Tung oil was first saponified with lime and then thermally cracked to yield a crude oil which was refined to produce diesel fuel and small amounts of gasoline and kerosene and it was found that 68 kg of the soap from the saponification of tung oil produced 50 L of crude oil.

Grossley et al. (1962) studied the temperature effect on the type of products obtained from heated glycerides. Catalysts have been used in many studies, largely metallic salts, to obtain paraffins and olefins similar to those present in petroleum sources. Soybean oil was thermally decomposed and distilled in air and nitrogen sparged with a standard ASTM distillation apparatus (Niehaus et al., 1986; Schwab et al., 1988). Schwab et al. (1988) used safflower oil as a high oleic oil control. The total identified hydrocarbons obtained from the distillation of soybean and high oleic safflower oils were 73-77 and 80-88%, respectively.

Catalytic cracking of vegetable oils to produce biofuel has been studied (Pioch et al., 1993). Coconut oil and palm oil stearin were cracked over a standard petroleum catalyst  $\text{SiO}_2/\text{Al}_2\text{O}_3$  at  $450^\circ\text{C}$  to produce gases, liquids and solids with lower molecular weights. The condensed organic phase was fractionated to produce biogasoline and

biodiesel fuels. The chemical compositions (heavy hydrocarbons) of the diesel fractions were found to be similar to fossil fuels.

## **2.2 Biodiesel Production using Ultrasonic Energy**

As of present, impeller mixing is the most widely used process in over 85 industrial scale biodiesel plants worldwide and at the same time, to enhance mixing one can use either ultrasound energy that can also produce high shear in the liquid medium. Applications of sonochemistry (which deals with the ultrasound energy) have been developed in virtually all areas of chemistry and related chemical technologies (Ertl, 2000). Ultrasound is the process of propagation of the compression (rarefaction) waves with frequencies above the range of human hearing (Benitez, 1999). It consists of the frequencies ranging from approximately 20 KHz to 10 MHz, with associated acoustic wavelengths in liquids of roughly 100 to 0.15 mm (not on the scale of molecular dimensions). Acoustic cavitation is the most important non linear phenomena due to ultrasound and its chemical effects. Acoustic cavitation is the formation, growth, and implosive collapse of bubbles in a liquid irradiated with sound or ultrasound. When sound passes through a liquid, it consists of expansion (negative pressure) waves and compression (positive pressure) waves. These cause bubbles (which are filled with both solvent and solute vapor and with previously dissolved gases) to grow and recompress. Under proper conditions, acoustic cavitation can lead to implosive compression in such cavities. Such implosive bubble collapse produces intense local heating, high pressures, and very short lifetime of bubbles, which causes the fast mixing. Cavitation is an extraordinary method of concentrating the diffuse energy of sound into a chemically

useable form (Ertl, 2000). Ultrasonication provides the mechanical energy for mixing and the required activation energy for initiating the transesterification reaction. Low-frequency ultrasonic irradiation is a useful tool for emulsification of immiscible liquids. The collapse of the cavitation bubbles disrupts the phase boundary and causes emulsification, by ultrasonic jets that impinge one liquid to another (Stavarache, 2005).

On the basis of the above principle, several biodiesel production processes have been developed. In one such study, base-catalyzed transesterification of vegetable oil was performed (Starvarache, 2003, 2005) using low frequency ultrasound (28-40 kHz). Previous studies reported excellent ester yields (98-99%) with a low amount of catalyst in a much shorter time than with mechanical stirring. Excellent yields of biodiesel were further observed (Colucci, 2005) in an alkaline catalyzed transesterification of soybean oil using ultrasonic mixing in a shorter time at three different levels of temperature and four different levels of alcohol-to-oil ratios. The rate constants of this reaction were found to be 3-5 times higher than those reported in the literature for mechanical mixing. This is because of the increase in interfacial area and activity of the microscopic and macroscopic bubbles formed when ultrasonic waves of 20 kHz were applied to a two-phase reaction system. In another experiment (Goldberg, 1966) the continuous alcoholysis of vegetable oils with ultrasonic vibrations (800-1200 cycles/s, irradiation intensity 1-2 W/cm<sup>2</sup>) resulted in an increased productivity (with or without catalysts) and an improved quality and color of the product without high- temperature treatment. It was reported that ultrasonic mixing had a significant effect on enzymatic transesterification as well. Ultrasonication showed higher (faster) transesterification rates (Shah, 2005; Wu,

2005) and higher operational stability for the enzymes, without changing the characteristics of the enzymes (Hielscher, 2005).

### **2.3 Solid Catalysis in Biodiesel Production**

The majority of the biodiesel production around the world is carried out by employing the homogeneous base catalyzed process because it is kinetically much faster than heterogeneously catalyzed transesterification and is economically viable. However, because of separation problems and product quality concerns, extensive research on heterogeneous catalysis towards the biodiesel production is ongoing all over the world.

In general the factors which govern the path of transesterification reactions are nature of raw materials, types of catalysts and optimum experimental conditions (temperature, oil to methanol ratio and catalyst concentration). As far as experimental condition is concerned for the generation of methyl ester with high yield, optimization of certain parameters or the application of optimized parameters are necessary. For example, a solid base catalyst, prepared under the specified conditions of 3.5 wt%  $\text{KNO}_3$  loadings on  $\text{Al}_2\text{O}_3$  substrate followed by calcinations at 773 K for 5 h produced the catalytic group of Al-O-K and favored the conversion of soybean oil in to methyl esters (Xie, 2006) with a FAME yield of more than 75%. Similarly, a heterogeneous base catalyst, Na/NaOH/ $\gamma$ - $\text{Al}_2\text{O}_3$ , employed under the optimized reaction conditions such as the reaction time, the stirring speed, and oil to methanol ratio explored the catalytic activity equal to homogeneous NaOH catalyst. The conversion rate was increased over two orders of magnitude to the homogeneous reaction with several of the zeolite catalysts when metals are considered as catalysts (Suppes, 2004). They recommended temperatures of 25-65 °C

and a catalyst concentration of 1-3% for optimum transesterification yields. Moreover they also observed the largest conversions taking place in sodium hydroxide and zirconium based catalysts and the use of immobilized lipase catalyst failed to produce methyl esters.

Demirbas (2003) revealed that the commonly accepted molar ratios of alcohol to glycerides for the transesterification of vegetable oils are 6:1-30:1. The change in catalyst-to-oil ratio under the reaction conditions of temperature of 650 °C, residence time 2.6 s and steam-to-oil weight ratio of 0.83 was explored. It was found that there was a slight increase in biodiesel production efficiency at the beginning stage and then, a decrease in biodiesel yield slightly thereafter which could be attributed to cracking of FAME at that higher temperature. The common reason for the change in the value of the catalyst-to-oil weight ratio is the change in contact conditions between oil and catalysts which in turn changes the average activation of catalysts. In general, as the catalyst-to-oil weight ratio increases, the probability of contact between oil and active centers also increases. Under these conditions, maximum transfer of energy is possible favoring easier transesterification.

Even though the role of homogeneous catalysts are significant for the industrial or large scale production of biodiesel and for easy conversion at moderate temperatures (40 to 65 °C), some of the major disadvantages in using such catalysts during transesterification are its soluble tendency into the reaction mixtures which prevents the separation process. It has been reported that (Certinkaya, 2004), the solubility of homogeneous catalysts either in biodiesel layer and or in glycerin layer is possible to a certain extent. Current methods such as bubble washing, spray washing, counter current



washing, and agitation are extensively used to wash and purify the contaminated products. However, these processes are considered time consuming and uneconomical. Besides, catalysts contaminated crude glycerol which is separated by gravitational settling or centrifuging and is valued low in present markets which compounds the seriousness of the separation issue.

Another problem associated with transesterification is the presence of water in the reaction mixture which causes the soap formation via saponification. An interesting remedial measure suggested (Filip, 1992) in relation of minimizing or preventing the soap formation is the use of 2 or 3 mol %  $K_2CO_3$ . The key role of  $K_2CO_3$  in this case is the formation of corresponding bicarbonate salt instead of water. Similarly during the production of non digestible polyol polyesters through interesterification of fatty acids with polyols, e.g. sucrose, several improvements, such as the application of low temperature and/or high pressure for increasing the mass transfer area, using back mixing in the initial stages, and plug-flow conditions in the final stages have been exercised.

As compared to homogenously catalyzed process, the transesterification with solid catalyst occurs at harsher reaction conditions i.e. at higher temperatures and pressures. This is because of the fact that the solid catalyzed process is a immiscible liquid/liquid/solid 3-phase system (corresponding to oil, methanol & catalyst)(Singh, 2007) that is highly mass transfer limited. In one study, supported solid catalysts CaO/MgO was used (Wang, 2005) for the transesterification of rapeseed oil at a relatively low temperature of 65°C by impregnating on a MgO support followed by calcination at 700°C in  $Ca(Ac)_2$  solution. The catalyst showed higher activity with a glycerol yield of more than 80 % purity. In other work (Serio, 2006) soybean oil was

transesterified at 100°C with methanol using MgO and calcined hydrotalcites (CHT) as catalysts. Four different basic sites were individuated at MgO and the calcined hydrotalcites for the transesterification and the strongest basic site was able to do the transesterification reaction below 100°C. More than 45 % of biodiesel yield was observed in case of MgO and more than 75 % yield was observed in case of CHT. It was reported that at a higher temperature of 200°C, more than 95 % of yield was observed for MgO and CHT catalysts. Biodiesel production with High Surface Area (HSA) nanocrystalline metal oxides on TiO<sub>2</sub>, MgO and CaO supports were investigated (Dean, 2006). M-Acetylacetonate (AcAc) was supported on the HSA support where M being Na, K, Ca, Li, V, Fe, N, and Al. The best catalysts tested were CaO and AcAc supported on MgO and TiO<sub>2</sub>.

In a different work biodiesel production of jatropha curcas (Zhu, 2006) oil with a solid catalyst CaO dipped in ammonium nitrate followed by calcination at 900°C showed an oil conversion of 93% at 70°C after 3.5 hrs of transesterification. The catalyst dosages and the oil to methanol ratio used in the study were 1.5 % and 9:1 respectively. In other work of soybean oil transesterification (Liu, 2007) with SrO as a heterogeneous catalyst, a yield in excess of 95 % was observed below 70°C within 30 min. A long catalyst lifetime of SrO was also investigated as it sustained the activity after repeated used for 10 cycles.

## **2.4 Kinetics of Transesterification**

Although the importance of biodiesel as an alternative fuel has grown during the last twenty years, the chemical kinetics of transesterification, very important for process

design, remain controversial. Kinetics describes the rate of chemical reactions. Rate equations are typically written in terms of the concentration of the reactants. In the past, it has been observed that the base catalyzed transesterification is a second order reaction (Darnoko, 2000). This has been confirmed in a different work for the transesterification of soybean oil with methanol using sodium hydroxide a homogeneous catalyst (Noureddini, 1997). In this work, it was assumed that transesterification is a three-step, reversible process, and the reaction rate constants and activation energies were determined for all the forward and reverse reactions.

In a different work, the rate constants and the reaction order were determined for each of the steps in the presence of a catalyst with a computerized kinetics program (Freedman, 1986). It was found that the forward reactions appear to be pseudo-1st order or 2nd order depending upon conditions used. Reverse reactions appeared to be 2nd order. At a MeOH/oil molar ratio of 6:1, a shunt reaction was observed. Activation energies were determined for all forward and reverse reactions under a variety of experimental conditions for plots of  $\log k$  vs.  $1/T$  (where  $k$  is the rate constant and  $T$  is the temperature).

## **2.5 Upgrading Biodiesel**

One major limitation of biodiesel is problems associated with cold flow and filter plugging due to oxidative instability. Oxidative instability arises as a result of the presence of unsaturation in the biodiesel (fatty acid methyl esters) and the cold flow problems are because the presence of saturation in the fatty acid methyl esters. Accordingly, research is ongoing by numerous groups to upgrade the biodiesel via

techniques including deoxygenation, hydrodeoxygenation, decarboxylation etc. in order to get rid of unsaturation and oxygen from fatty acid methyl esters. Although upgrading of biodiesel has not received much of attention, this is an important parameter that needs to be resolved before widespread commercialization of biodiesel, especially in regions prone to colder climates. Following are some work that has been done in this regard.

The behavior of HZSM-5 zeolite in the upgrading of wood pyrolysis oil produced in the fast-pyrolysis plant was studied (Vitolo, 1999, 2000) in repeated upgrading-regenerating cycles. As a consequence of the catalytic process, coke and tar were also formed as undesirable by-products. The continued regeneration of the zeolite by air at 500°C, reduced the effectiveness of the catalyst in converting biomass pyrolysis oils to an aromatic product. Finally, an irreversible deactivation was observed. Even if the regeneration was conducted at 500°C, localized raisings of temperature above 500°C due to the combustion of coke caused dehydroxylation of the Bronsted acid sites that predominate in zeolites activated at 500°C with formation of Lewis acid sites. Thus, the active acid sites in the upgrading reactions are presumed to be preferentially Bronsted acid sites, which were gradually deactivated by the repeated regeneration treatments.

In a different work (Fernandes, 2006) a method for the reduction of esters using a high oxidation state oxo-complex as a catalyst was reported. The system silane/MoO<sub>2</sub>Cl<sub>2</sub> (5 mol %) proved to be very efficient for the reduction of aliphatic and aromatic esters to the corresponding alcohols in good yields.

Elimination of oxygen from carboxylic groups was studied (Senol, 2005) with model compounds, methyl heptanoate and methyl hexanoate, on sulphided NiMo/g-Al<sub>2</sub>O<sub>3</sub> and CoMo/g-Al<sub>2</sub>O<sub>3</sub> catalysts in a flow reactor. Catalyst performances and reaction

schemes were addressed. Carboxylic acid was further converted to hydrocarbons either directly or with an alcohol intermediate. Decarboxylation of the esters led to hydrocarbons in the third path. No oxygen containing compounds were detected at complete conversions. However, the product distributions changed with time, even at complete conversions, indicating that both catalysts deactivated under the studied conditions.

In a different study (Kuvickova, 2005), deoxygenation reaction of vegetable oils over a carbon-supported metal catalyst was studied as a suitable reaction for production of diesel fuel-like hydrocarbons. Stearic acid, ethyl stearate, and tristearine have been used as model compounds. Catalytic treatment of all the three reactants resulted in production of n-heptadecane as the main product with high selectivity.

On the basis of the literature review, it was imperative that more work is needed to be done to find a robust enough solid catalysts selective towards transesterification. This work also was targeted towards finding an effective catalyst that could increase the oxidative stability and/or cold flow properties of biodiesel.

## CHAPTER III

### MATERIALS AND METHODS

This chapter discusses the materials and methods used in this study. Section 3.1 depicts materials and methods used in ultrasonic processing of triglycerides to produce biodiesel. Section 3.2 presents the material and methods used in the catalyst screening studies and section 3.3 describes the methodologies used in the catalyst characterization. Principles and methods used during transesterification kinetics study have been discussed in section 3.4. Finally, Section 3.5 discusses the principles of and methods used for the thermodynamic analysis and the deoxygenation studies of biodiesel.

#### **3.1 Biodiesel Production Using Ultrasonication**

In the present study, the transesterification of soybean oil using potassium hydroxide as an alkaline catalyst was performed with an ultrasonic processor. This processor used electric excitation to generate ultrasound, which was transmitted into the liquid sample via a sonotrode that caused mixing and provided the necessary energy for the transesterification. The main aim of this research was to find the effects of the wave amplitudes and reaction time (and hence, total energy input and temperature) on the yield of biodiesel.

### **3.1.1 Reagents and materials**

Solvent-extracted degummed soybean oil was purchased from Bunge Corporation (Marks, MS, USA). Potassium hydroxide (99 %) was purchased from Sigma- Aldrich, (St. Louis, MO, USA)., and used as a catalyst for the reaction. Methanol (99.9%) was purchased from Fisher Scientific (Hampton, NH, USA.).

### **3.1.2 Equipment**

An ultrasonic processor (UP400S, Hielscher, Ringwood, NJ, U.S.A.) was used to perform the transesterification reaction. The equipment consisted of the processor, the sonotrode, and the PC control (UPC400T). The processor operated at 400 W and 24 kHz frequency. The amplitude and the pulse for the reaction were adjustable from 20 to 100% and from 0 to 100%, respectively. The titanium sonotrode (H22D) with a diameter of 22 mm and a length of 100 mm was used to transmit the ultrasound into the liquid. Using the PC control, the process parameters such as amplitude, pulse, and operating time were modulated. The control system automatically recorded the actual energy input and resultant temperature variation.

### **3.1.3 Transesterification**

A mixture of 25 ml of methanol and 1 g of potassium hydroxide was agitated using a magnetic stirrer for 5 min to form the methoxide and then 100 ml of Soybean oil was mixed with the previously prepared potassium methoxide (1:6 molar ratio) in a conical flask. Then, the mixture was transferred to the reaction chamber to be subjected to ultrasound waves. The sonotrode was submerged up to 25 mm into the solution. The

amplitude and time of the reaction were adjusted by the PC controller. The four different amplitudes were 25%, 50%, 75%, and 100%, and the four different durations were 5, 10, 15, and 20 min. The pulse of the reaction was kept constant for all combinations at 100%. All the combinations were tested with three replicates. After completion of the reaction, the solution was treated with concentrated sulfuric acid in order to neutralize the potassium hydroxide and to immediately stop the reaction. The product, a mixture of fatty acid methyl esters (FAME's) and glycerol, was then transferred to a freezer (-5°C) before sending it for gas chromatography (GC) analysis.

#### **3.1.4 Gas chromatography analysis**

Samples obtained from the top layers of the mixture (after stabilization) were sent for GC analysis. The analysis was done with GC6890N (Agilent Technologies, Inc., Santa Clara, CA) with FID connected to a Solgel premium capillary column (30 m × 0.25 mm × 0.25 μm), and with MSD connected to HP-5MS column (30 m × 0.25 mm × 0.25 μm). Quantification analysis utilized FID. The oven was first held at 190 °C for 2 min, and then ramped to 214 °C at a rate of 3 °C/min. The injection volume was 0.2 μL, and split ratio was 100/1. The inlet temperature was 250 °C, and the detector temperature was 270 °C. Samples were added with methyl undecanoate (≥ 99%) as the internal standard, and diluted with chloroform (Assay 100%, HACH Company, Loveland, CO). Calibration employed ethyl palmitate (≥ 99%), ethyl stearate (≈ 99%), ethyl oleate (98%), ethyl linoleate (≥ 99%), and ethyl linolenate (≥ 98%).



## **3.2 Biodiesel Production with Solid Catalysts**

### **3.2.1 Reagents and materials**

Solvent-extracted degummed soybean oil donated by Bungi Corporation (Marks, MS, USA) was used as the triglyceride. The solid catalysts (PbO, PbO<sub>2</sub>, Pb<sub>3</sub>O<sub>4</sub>, MgO, ZnO, CaO, Ti<sub>2</sub>O<sub>3</sub>, MnO<sub>2</sub>, BaO and CaO) and methanol (99.9 %) used in the study were purchased from Sigma Aldrich (St-Louis, MO, USA) and Fisher Scientific (Hampton, NH, USA).

### **3.2.2 Preparation of mixed metal oxides**

From equation 1.1 to 1.4 it is clear that sodium is responsible for the transesterification of soybean oil with NaOH. Wen et. al. (1996) incorporated sodium on lithium oxide and alumina in order to prepare a layered double hydroxide. From our preliminary study with alumina towards transesterification we found that alumina is not a good catalyst towards transesterification whereas lanthanum has a positive effect towards transesterification. So we incorporated sodium on lithium and lanthanum to get a solid mixed oxide catalyst. In order to prepare this catalyst a mixture of 0.1 moles of lithium hydroxide, 0.2 moles of sodium hydroxide and 0.05 moles of lanthanum oxide in 150 ml of distilled water were treated hydrothermally at four different temperatures of 25, 100, 150 and 200 °C (labeled as 25°C - NaMO1, 100°C - NaMO2, 150°C - NaMO3 and 200°C - NaMO4) in a high pressure batch reactor for 10 h followed by vigorous mixing at room temperature for the next 10 h. The prepared catalysts were washed thoroughly with

distilled water until the pH reached and was maintained at 7.0. Then, the catalysts were calcined at 500°C.

### **3.2.3 Preparation of layered double hydroxides (LDH)**

A drop wise solution of 37.5 g of  $\text{Al}(\text{NO}_3)_2 \cdot 9\text{H}_2\text{O}$  in 250 ml of distilled water was added to a mixture of 78.3 g of lithium hydroxide ( $\text{LiOH} \cdot \text{H}_2\text{O}$ ) and 5.1 g of  $\text{Na}_2\text{CO}_3$  in 600 ml of distilled water at room temperature with vigorous mixing (Shumaker, 2007). Then, the catalyst was aged for 24 hrs overnight at 75°C followed by Centrifuging/Decanting/Washing. The prepared catalysts were washed thoroughly with distilled water in order to maintain  $\text{P}_\text{H} = 7$  and finally the catalysts were dried at 105°C and calcined at 450°C for 2 hrs. This catalyst was labeled as LiLDH.

### **3.2.4 Equipment**

The transesterification with all the solid catalysts was carried in a fully automated high-pressure high-temperature batch reactor (PARR Instrument, 4843, Moline, Illinois, USA). The equipment consists of a high pressure cylindrical chamber, a heater, a water line (in order to control the temperature) and a stirrer.

### **3.2.5 Transesterification of soybean oil**

A mixture of 30 ml methanol and 100 ml of soybean oil (equivalent to 7:1 molar ratio) was prepared using a magnetic stirrer and then 2 g of solid catalyst was added into the high pressure reaction vessel. Three different temperatures of 75, 150 and 225°C was selected for the comparison of the biodiesel (FAME) yield. The transesterification was

done at the selected temperature for 2 hours and then the products were separated, frozen and sent for gas chromatography (GC) analysis. The products were frozen in order to terminate the transesterification reaction.

### **3.2.6 Transesterification for kinetics analysis**

Two different methods of transesterification were followed for the kinetics analysis of metal oxides and mixed metal oxides. For some of the catalysts, (PbO, MgO, MnO<sub>2</sub>, NaMO1, NaMO2, NaMO3 and NaMO4), the mixture (oil, methanol and catalyst) was first heated to 215 °C (it was found that there was only slight conversions ranging from 3 to 4 % during the ramping period). Then the reaction was carried out for 2 hours in the high-pressure reactor. Samples were taken out in 15-minute intervals and the fatty acid methyl esters yield was measured with gas chromatography. For the last two catalysts, (CaO and BaO), it was observed that significant conversions took place during the first few minutes of the reaction (46 % and 20 %, respectively) while ramping up the temperature to 215 °C. Accordingly, the method was changed for these two experimental units. In this case, the oil was first heated with the catalyst to 215 °C, and then 30 ml of methanol was injected using a HPLC pump at a flow rate of 10 ml/min for 3 minutes. Then, the experiments were carried out for the next 14 minutes at a sampling interval of 2 minutes. The product (a mixture of fatty acid methyl esters and glycerol) was separated and then transferred to a freezer before being sent for gas chromatography (GC) analysis.

### **3.2.7 Gas chromatography analysis**

The top layer of each sample, after stabilization, was analyzed for FAME composition at the Mississippi State Chemical Laboratory, Mississippi State University, with gas chromatography (methods mentioned in section 3.1.4).

## **3.3 Catalyst Characterization**

### **3.3.1 Determination of surface area of the catalysts**

Surface area of the metal oxides was measured with multipoint Brunauer, Emmett and Teller (BET) method from the Quantachrome Surface Analysis Instrument (Autosorb 1-C, Boynton Beach, Florida, USA). This was done using nitrogen adsorption/desorption isotherms at liquid nitrogen temperature and relative pressures ( $P/P_0$ ) ranging from 0.04-0.4 where a linear relationship was maintained.

### **3.3.2 Determination of acid/base strength**

Site strength refers to the relative tendency of an acid or base to donate or accept a proton. The strength of acid and bases can be compared by their reaction with water. Acidic and basic site strengths of each of the metal oxides were determined (Xie, 2006) by basic and acidic Hammett indicators respectively. Approximately 50 mg of sample was shaken with 1 ml of a solution of Hammett indicator diluted in benzene and methanol for basic and acidic tests respectively and left to equilibrate for two hours. The color of the catalyst was then noted. The basic Hammett indicator (for acid site strength)

used were: Neutral red ( $pK_a=6.8$ ), Methyl red ( $pK_a=4.8$ ), P-dimethylaminoazobenzene ( $pK_a=3.3$ ) and Crystal violet ( $pK_a=0.8$ ). The acidic Hammett indicators (for base site strength) used were: Phenolphthalein ( $pK_{BH^+}=8.2$ ), Nile blue ( $pK_{BH^+}=10.1$ ), Tropaeolin ( $pK_{BH^+}=11$ ), 2,4-dinitroaniline ( $pK_{BH^+}=15$ ), 4-chloro-2-nitroaniline ( $pK_{BH^+}=18.2$ ) and 4-chloroaniline ( $pK_{BH^+}=26.5$ ). The  $H_0$  value of a sample at acid site was determined by the smallest  $H_0$  value among the Hammett indicators which has been subjected to a color change and which had the  $H_0$  value less than 7.0. And the  $H_0$  value of a sample at the base site was determined by the greatest  $H_0$  value among the Hammett indicators which had been subjected to a color change and having  $H_0$  value more than 7.0.

### **3.3.3 Determination of acidity /basicity**

A common method for evaluating the basicity of a base is to report the acidity of the conjugate acid and vice versa for the acidity. In our case, the method of titration was used (Zhu, 1999) to determine the acidity/basicity of the catalysts. For Basicity, the basic catalyst was mixed with a known concentration of HCl. The basic catalyst will neutralize HCl by an equivalent amount to its basicity. As a result, the original concentration of HCl will be reduced. The resultant concentration of HCl was determined by titration with NaOH and finally the adsorbed amount of HCl on the catalyst was determined. In retrospect, for acidity determination, an acidic catalyst was mixed with a known concentration of NaOH and the amount of NaOH adsorbed to the catalysts was determined via titration with HCl. For amphoteric catalysts both acidity as well as basicity was determined.

### 3.3.4 X- ray Diffractogram and Scanning Electron Microscope analysis

X- ray diffraction images, SEM and elemental analysis images were analyzed in the Electron Microscopic Center, Mississippi State University for Different layered double hydroxides and mixed oxides.

In the X-ray analysis the powder of NaMO catalysts was identified by X-ray diffraction with Rigaku III X-ray diffraction system using  $\text{CuK}_\alpha$  (40 kV/ 44 mA) radiation ( $\lambda = 0.8 \text{ nm}$ ) and a scanning rate of  $1^\circ \text{ min}^{-1}$ . The pattern was over the range of  $10^\circ < 2\theta < 90^\circ$ .

In the SEM analysis with LaB6 emitter system at Mississippi State University, electrons are thermionically emitted from a tungsten or lanthanum hexaboride ( $\text{LaB}_6$ ) cathode and are accelerated towards an anode. Tungsten was used because it has the highest melting point and lowest vapor pressure of all metals, thereby allowing it to be heated for electron emission. The electron beam, had an energy range of 0-5 keV, was focused by a condenser lenses into a beam with a very fine focal spot sized of  $60 \mu\text{m}$ . Standard used in this analysis were  $\text{CaCO}_3$ ,  $\text{SiO}_2$ , Pure Aluminum and  $\text{LaB}_6$ .

### 3.4 Kinetics of Transesterification

The transesterification reaction is a reversible reaction and therefore, excess methanol is used to drive the reaction forward. Equation 3.1 shows the generalized transesterification reaction, where A is the triglyceride, B is methanol, C is FAME and D is glycerol. The equation also shows the stoichiometric relationship between the reactants and the products.



The general rate equation for the Equation 3.1 will be,

$$-\frac{dC_A}{dt} = kC_A^\alpha C_B^\beta \quad (3.2)$$

Where,

$$-\frac{dC_A}{dt} = \text{the consumption of reactant A per unit time}$$

$k$  = rate constant

$C_A$  = concentration of A after time  $t$

$C_B$  = concentration of B after time  $t$

$\alpha$  = reaction order of reactant A

$\beta$  = reaction order of reactant B

Also,

$$C_A = C_{A0}(1-X) \quad (3.3)$$

$$C_B = C_{A0}(\theta_B - 3X) \quad (3.4)$$

$$\theta_B = C_{B0} / C_{A0} \quad (3.5)$$

Where,

$C_{A0}$  = initial concentration of A

$C_{B0}$  = initial concentration of B

$X$  = conversion

$\theta_B$  = the ratio of  $C_{B0}$  to  $C_{A0}$

Equation 3.2 can be written as

$$\frac{dX}{dt} = kC_{A0}^{(\alpha+\beta-1)}(1-X)^\alpha(\theta_B - 3X)^\beta \quad (3.6)$$

In the present work, 8 different cases were analyzed in order to get the reaction order. These case were,

$$(\alpha=0, \beta=0); (\alpha=1, \beta=0); (\alpha=0, \beta=1); (\alpha=1, \beta=1); (\alpha=2, \beta=0);$$

$$(\alpha=0, \beta=2); (\alpha=2, \beta=1); (\alpha=1, \beta=2).$$

For each case, definite integrals of Equation 3.6 were calculated from a conversion of X=0 to a conversion of X=X in the time span of t = 0 to t = t. Then the calculated equation for each case was transferred into a linier equation passing through origin (y=mx). The transferred equations for all the 8 cases are as follows:

Case 1: ( $\alpha=0, \beta=0$ )

$$C_{A0}X = kt \quad (3.7)$$

Case 2: ( $\alpha=1, \beta=0$ )

$$\ln\left(\frac{1}{1-X}\right) = kt \quad (3.8)$$

Case 3: ( $\alpha=0, \beta=1$ )

$$-\frac{1}{3}\left[\ln\left(\frac{\theta_B - 3X}{\theta_B}\right)\right] = kt \quad (3.9)$$

Case 4: ( $\alpha=1, \beta=1$ )

$$\frac{1}{(\theta_B - 3)} \ln\left[\frac{(\theta_B - 3X)}{(1-X)\theta_B}\right] = kC_{A0}t \quad (3.10)$$

Case 5: ( $\alpha=2, \beta=0$ )

$$\frac{X}{(1-X)} = kC_{A0}t \quad (3.11)$$



Case 6: ( $\alpha=0, \beta=2$ )

$$\frac{X}{(\theta_B - 3X)\theta_B} = kC_{A0}t \quad (3.12)$$

Case 7: ( $\alpha=2, \beta=1$ )

$$\frac{1}{(\theta_B - 3)} \left\{ \frac{X}{(1-X)} - \frac{3}{(\theta_B - 3)} \ln \left[ \frac{(\theta_B - 3X)}{(1-X)\theta_B} \right] \right\} = kC_{A0}^2t \quad (3.13)$$

Case 8: ( $\alpha=1, \beta=2$ )

$$\frac{1}{(3 - \theta_B)} \left\{ \frac{3X}{(\theta_B - 3X)\theta_B} - \frac{1}{(3 - \theta_B)} \ln \left[ \frac{(1-X)\theta_B}{(\theta_B - 3X)} \right] \right\} = kC_{A0}^2t \quad (3.14)$$

For Equations 3.7 through 3.14, if it is assumed that the left side component is an ordinate (y variable) and  $t$  (for eq. 3.7 to 3.9),  $C_{A0}t$  (for eq. 3.10 to 3.12) and  $C_{A0}^2t$  (for 3.13 to 3.14) are abscissas (x variable) respectively, the equations are in the form of  $y=mx$  (a straight line passing through origin). For all 8 cases, the y variable was plotted against the corresponding x variable and the coefficient of determination ( $R^2$ ) was determined. In all the cases (Eq. 3.7 to 3.14), the slope of the straight line is the rate constant ( $k$ ) for the reaction. The highest  $R^2$  for each case was observed and the case that gave the highest  $R^2$  was used to determine the reaction order.

### 3.5 Biodiesel Upgrading

This section presents the principles of thermodynamic analysis and the methods used for biodiesel deoxygenation.

### 3.5.1 Thermodynamic analysis

The thermodynamic analysis was done in order to predict the amount of deoxygenated product. The second law of thermodynamics says that a mixture of chemicals satisfies its chemical equilibrium state (at constant temperature and pressure) when the free energy of the mixture is reduced to a minimum. Therefore the composition of the chemicals satisfying its chemical equilibrium state can be found by minimizing the function of the free energy of the mixture. Gibbs energy of formation is important in the analysis of chemical reactions. Values for individual compounds are required to determine the change in Gibbs energy of reaction. If the change in Gibbs energy is negative, the thermodynamics for the reaction are favorable. On the other hand, if the change in Gibbs energy is highly positive, the thermodynamics for the reaction are not favorable. So if

$$\Delta G_{\text{reaction}} < 0 \text{ kjoule/mol} \quad [\text{reaction favorable}]$$

$$0 < \Delta G_{\text{reaction}} < 50 \text{ kjoule/mol} \quad [\text{reaction possibly favorable}]$$

$$\Delta G_{\text{reaction}} > 50 \text{ kjoule/mol} \quad [\text{reaction not favorable}]$$

If the pressure and the temperature of the system are constant, the equilibrium of the system is given as follows (Denbigh, 1966):

$$dG = \sum_{i=1}^K \mu_i dn_i \quad (3.15)$$

Where  $\mu_i$  and  $n_i$  are the chemical potential and the number of moles of species  $i$ , respectively.  $K$  is the total number of chemical species in the reaction mixture.

The objective is to find the set of  $n_i$ 's which minimize the value of  $G$ . This can be solved in two ways (Smith and Missen, 1982): (i) stoichiometrically and (ii) non-stoichiometrically. In the stoichiometric approach, the system is described by a set of stoichiometrically independent reactions, and they are typically chosen arbitrarily from a set of possible reactions (Fishtik, 2000). In contrast, with the non-stoichiometric approach the equilibrium composition is found by the direct minimization of the Gibbs free energy for a given set of species (Win, 2000). The advantages of non-stoichiometric approach over the stoichiometric approach are as follows (García and Laborde, 1991): (a) a selection of the possible set of reactions is not necessary, (b) no divergence occurs during the computation, and (c) an accurate estimation of the initial equilibrium composition is not necessary. The non-stoichiometric approach has been used in this study. Eq. 3.15 can be written as follows:

$$G = \sum_{i=1}^K \mu_i n_i \quad (3.16)$$

To find the  $n_i$  that minimize the value of  $G$ , it is necessary that the values of  $n_i$  satisfy the elemental mass balances as given in Eq. 3.17.

$$\sum_{i=1}^K a_{li} n_i = b_l, \quad l=1, \dots, M \quad (3.17)$$

where  $a_{li}$  is the number of gram atoms of element  $l$  in a mole of species  $i$  and  $b_l$  is the total number of gram atoms of element  $l$  in the reaction mixture.  $M$  is the total number of atomic elements.

Eq. 3.16 can be further expressed as (Lwin et al. 2000; Vasudeva et al. 1996):

$$G = \sum_{i=1}^K n_i \Delta G_i^0 + RT \sum_{i=1}^K n_i \ln y_i + RT \sum_{i=1}^K n_i \ln P \quad (3.18)$$

where  $\Delta G_i^0$  is the standard Gibbs free energy of formation of species  $i$ .  $R$  is the universal gas constant and  $T$  is the temperature.  $y_i$  is the mole fraction of species  $i$  and  $P$  is the total pressure of the system.

At low pressure and high temperature, the system can be considered as ideal (Lwin et al. 2000; Vasudeva et al. 1996). The objective function (3.18) was minimized using PROC NLP in SAS 9.1. It was also solved by the Lagrange's multiplier method using SAS 9.1 while satisfying the elemental mass balances as given in Eq. 3.17. As entry data the program needs pressure, temperature, number of compounds, number of atoms, values of the Gibbs free energy of formation, and initial guesses for  $n_i$ 's in the equilibrium. Thermodynamic data were obtained from Yaws (1999).

### **3.5.2 Materials and methods used in deoxygenation of Biodiesel**

Two different experiments were carried out in order to upgrade biodiesel. The first one was the conversion of esters to the corresponding alcohols, a fundamental process in organic synthesis, which has gained renewed interest due to the need of converting fatty acid esters and other natural carboxylic acid derivatives into fuels or chemical feedstocks (Fernandes et. al., 2006). In this experiment methyl linoleate was used for the analysis since the soybean oil contains around 55-60% of methyl linoleate. To a solution of  $\text{MoO}_2\text{Cl}_2$  (5% mol) in dry toluene (5 ml) was added the ester (1.0 mmol) and phenyl silane ( $\text{PhSiH}_3$ , 2.0 mmol) under nitrogen atmosphere. The reaction mixture was stirred at reflux temperature of  $115^\circ\text{C}$  for 20 h. After evaporation, the reaction mixture was purified by silica gel column chromatography with the appropriate mixture

of *n*-hexane and toluene. Then, the sample was sent to the Mississippi State Chemical Laboratory, Mississippi State University for the mass spectrometric analysis.

The second experiment in order to upgrade the biodiesel was carried out with HZSM-5 zeolite (Calcined ZSM at 450°C for 4 hrs). 100 ml of pure biodiesel was mixed with 2 g of HZSM-5 catalyst in a high pressure reactor (Parr reactor) at three different temperatures of 215, 315 and 375°C for 10 hrs. Finally the product was centrifuged at 4050 rpm for 15 min in order to separate the catalyst out of mixture and then the samples were analyzed with mass spectrometer.

## CHAPTER IV

### RESULTS AND DISCUSSION

This chapter discusses the results and discussions of the present study. Section 4.1 presents the results pertinent to the ultrasonic processing study. Section 4.2 depicts the catalyst screening results. Catalyst characterization results have been described in Section 4.3. Section 4.4 shows the results of kinetic analysis followed by the reactor modeling. Finally Section 4.5 presents the results associated with upgrading biodiesel and fatty acid methyl esters.

#### **4.1 Ultrasonic Processing for Biodiesel Analysis**

In order to compare the results from ultrasonication, a control study was done without the application of ultrasonication. And it was found that for 100 ml of soybean oil and 25 ml of methanol with 1 g of KOH, took almost 1 hr for the transesterification for a FAME yield of 99%.

The above result of control sample was compared with the results from application of ultrasonication, and it was found that the application of ultrasonication was able to produce same amount of FAME yield in 5 min. Figure 4.1, 4.2 and 4.3 depicts overlaid images of biodiesel yield, input energy and reactant temperature variation with sonic amplitudes and time. The biodiesel yield (FAME %) from gas chromatography analysis showed a large variation due to the change in amplitude and reaction time (the

combination). The data collected from GC analysis showed a high yield of biodiesel (up to 99.34%) in a seemingly short time.

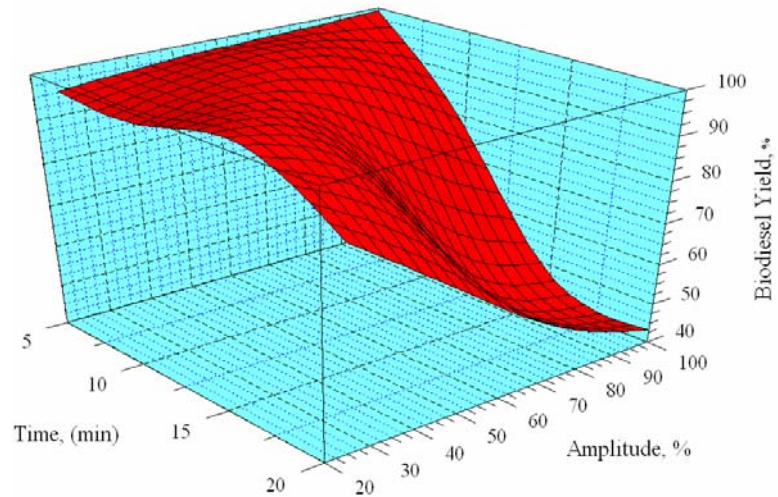


Figure 4.1 FAME yield variations with time and sonic wave amplitude

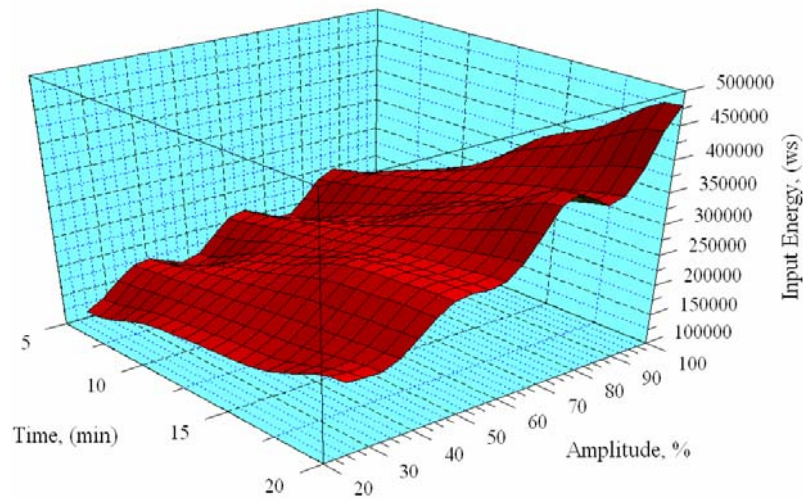


Figure 4.2 Input energy variations with time and sonic wave amplitude

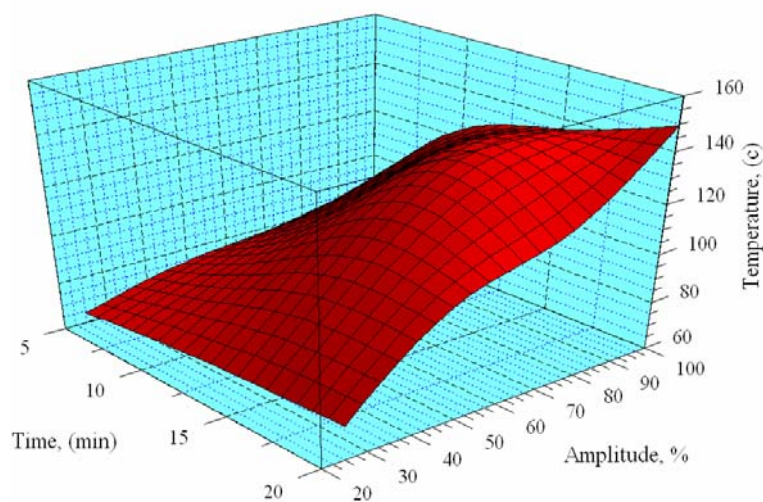


Figure 4.3 Temperature variations with time and sonic wave amplitude

#### 4.1.1 Effect of amplitude

The amplitude of sound waves had a large effect on the transesterification reaction. To better explain the results, data on input energy, temperature and yield for slices across Figure 4.1, 4.2 and 4.3 at 5 min, 10 min, 15 min and 20 min are depicted in Table 4.1.

At 5 min after the initiation of the reaction, it was clearly established that increasing wave amplitude resulted in an increase in reaction temperature as well as biodiesel yields. At the 100 % amplitude level, the ester yield was more than 99 % (highest in all the 16 amplitude-sonication time treatment combinations) and the corresponding input energy and temperature was 131177 J and 89°C, respectively (Table 4.1).



Table 4.1 Effects of amplitude, reaction time on yield of biodiesel via ultrasonication

| <b>Amplitude, %</b> | <b>Reaction time, min</b> | <b>Input energy, J</b> | <b>Temperature, °C</b> | <b>Yield, %</b> |
|---------------------|---------------------------|------------------------|------------------------|-----------------|
| 25                  | 5                         | 79538                  | 64                     | 95              |
| 50                  | 5                         | 91039                  | 74                     | 97              |
| 75                  | 5                         | 125201                 | 79                     | 98              |
| 100                 | 5                         | 131177                 | 89                     | 99              |
| 25                  | 10                        | 147022                 | 69                     | 95              |
| 50                  | 10                        | 214951                 | 91                     | 97              |
| 75                  | 10                        | 216911                 | 107                    | 91              |
| 100                 | 10                        | 274085                 | 124                    | 77              |
| 25                  | 15                        | 151975                 | 72                     | 99              |
| 50                  | 15                        | 303461                 | 110                    | 88              |
| 75                  | 15                        | 325500                 | 136                    | 58              |
| 100                 | 15                        | 409828                 | 136                    | 47              |
| 25                  | 20                        | 236971                 | 74                     | 87              |
| 50                  | 20                        | 310414                 | 107                    | 69              |
| 75                  | 20                        | 464485                 | 120                    | 52              |
| 100                 | 20                        | 546569                 | 149                    | 43              |

Also all four amplitudes generated greater than 95% biodiesel yield in 5 min.

Subjecting ultrasonication for 10 min produced high ester yields only at lower amplitudes. For example, an increase in amplitude from 25 to 50 % resulted in an ester

yield increase from 95 to 97%. However, at higher amplitudes, ester yields reduced drastically. This might be possible because of cracking followed by oxidation of the fatty acid methyl esters to aldehydes, ketones and lower chained organic fractions. It was observed that the ester yields were maximized at an optimum energy level. Similar trends were observed for 15 min and 20 min of ultrasonication at different amplitude levels.

#### 4.1.2 Effect of input energy

The data for input energy (i.e. sound energy) and yield of FAME's are shown in Fig. 4.4. According to the Fig. 4.4, it is evident that as the input energy increased, the FAME yield increased, reaches a maximum and started to decline. The reduction of FAME yield was attributed to thermal cracking. It was observed that in order to obtain biodiesel yields above 97%, the range for input energy to the transesterification should be maintained between 1.40 to 2.41 kJ/g of soybean oil.

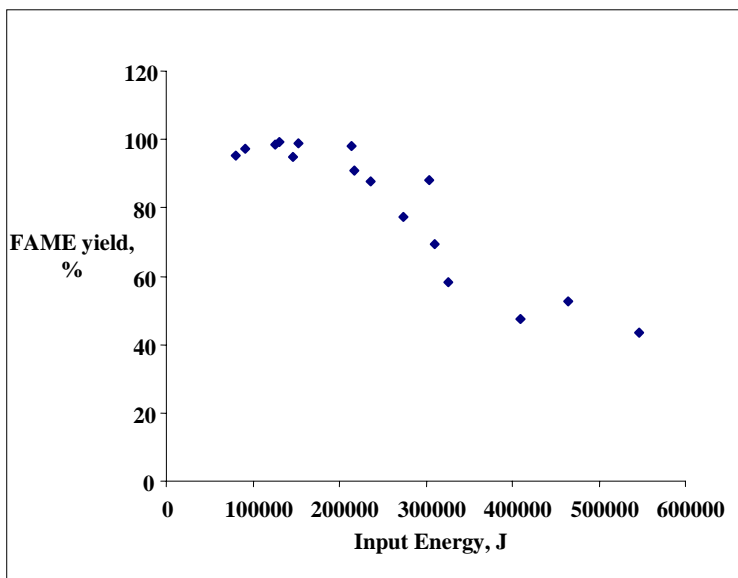


Figure 4.4 Effect of input energy on the fatty acid methyl esters yield.

## 4.2 Biodiesel Production with Solid Catalysts

### 4.2.1 Transesterification with metal oxides

The FAME yield after transesterification varied significantly among the catalysts tested. Also, there was a diverse response to temperature variations among different catalysts. Fig. 4.5 depicts the biodiesel (FAME) yield for all the catalysts (MgO, CaO, PbO, PbO<sub>2</sub>, Pb<sub>3</sub>O<sub>4</sub>, ZnO and Ti<sub>2</sub>O<sub>3</sub>) at three different temperatures of 75, 150 and 225°C. MgO and Pb<sub>3</sub>O<sub>4</sub> showed an increasing trend with increased temperature. Initially, at 75°C, both of them had an insignificant FAME yield (less than 5%), however, at higher temperatures (at 215°C), the yield was increased to 74 and 89%, respectively. The FAME yield of Ti<sub>2</sub>O<sub>3</sub> and ZnO peaked around 150°C and showed a precipitous decline at 225°C. This may be attributed to cracking of esters at higher temperatures.

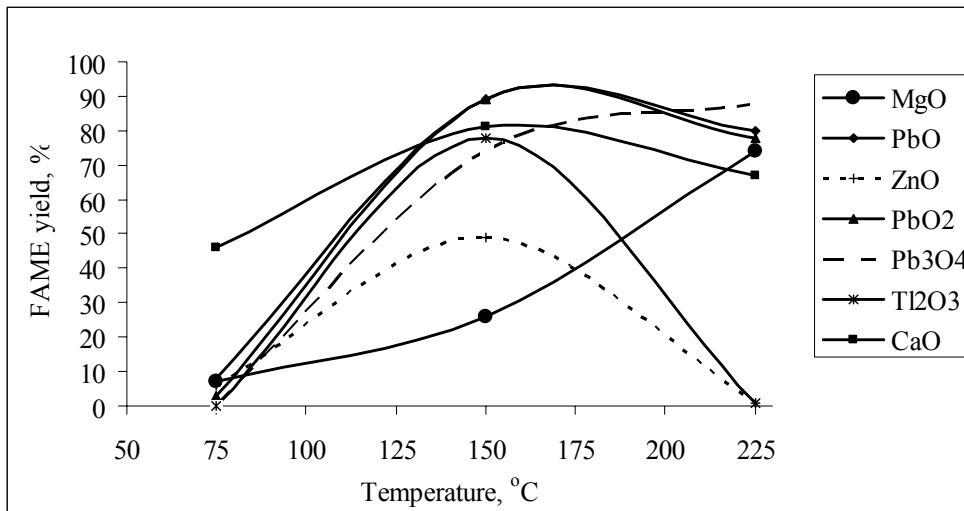


Figure 4.5 FAME yield with different solid catalysts

This observation is further reinforced by the fact that the resultant product looked much darker than in color than samples that had higher FAME yields. PbO and PbO<sub>2</sub> showed almost an identical trend at all the three temperatures tested. A maximum FAME yield of 89 % was observed for both catalysts at 150°C. The only difference in Pb<sub>3</sub>O<sub>4</sub> was that the increasing FAME yield trend sustained even beyond 225°C. Lead oxides, by far were the most potent for transesterification from all the oxide catalysts tested. It was interesting to note that CaO has displayed a different trend to the other catalysts. CaO was selective towards transesterification at all the temperatures tested and gave FAME yields of 46, 81 and 67 % at 75, 150, and 225°C respectively.

Figure 4.6 shows the biodiesel (FAME) yield for all the catalysts, PbO, MgO, MnO<sub>2</sub>, BaO and CaO, over 2 hours of transesterification. For PbO the yield was found to be more than 84 % after 1 hour, for MgO the maximum yield was found to be approximately 66% after 2 hours and for MnO<sub>2</sub> the yield surpassed 80 % after 2 hours.

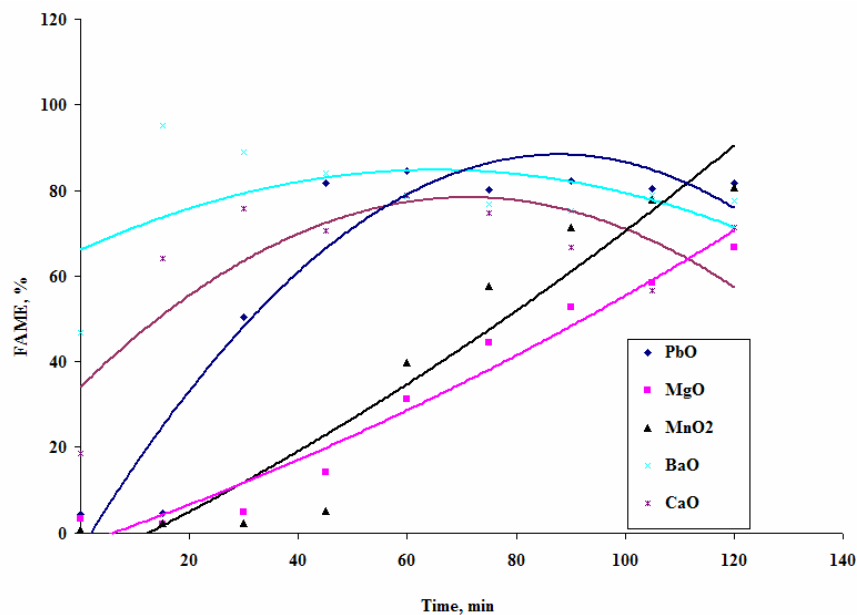


Figure 4.6 FAME yield for PbO, MgO, MnO<sub>2</sub>, BaO and CaO (reaction times denoted represent time after reactants reached 215°C)

For BaO and CaO, biodiesel yield was found to be more than 95% and 75% within 15 and 30 min respectively. Cracking of the methyl esters was observed subsequent to these time periods. The initiation of reduction of methyl esters yield could be attributed to the pretense that the rate of cracking exceeded the rate of transesterification for BaO and CaO after 15 and 30 minutes respectively under the provided reaction conditions. As a result, only 2 data points for BaO and 3 data points for CaO were at hand to calculate the reaction order and rate constant - which was not sufficient (Figure 4.6). Consequently, in order to capture the trend, the method was modified for these two catalysts. The data was collected in 2 min intervals for 14 minutes after attaining a temperature of 215 °C. The FAME yield for the BaO catalyst surpassed 85 % after 14 minutes and 78% for catalyst CaO after 2 min (figure 4.7).

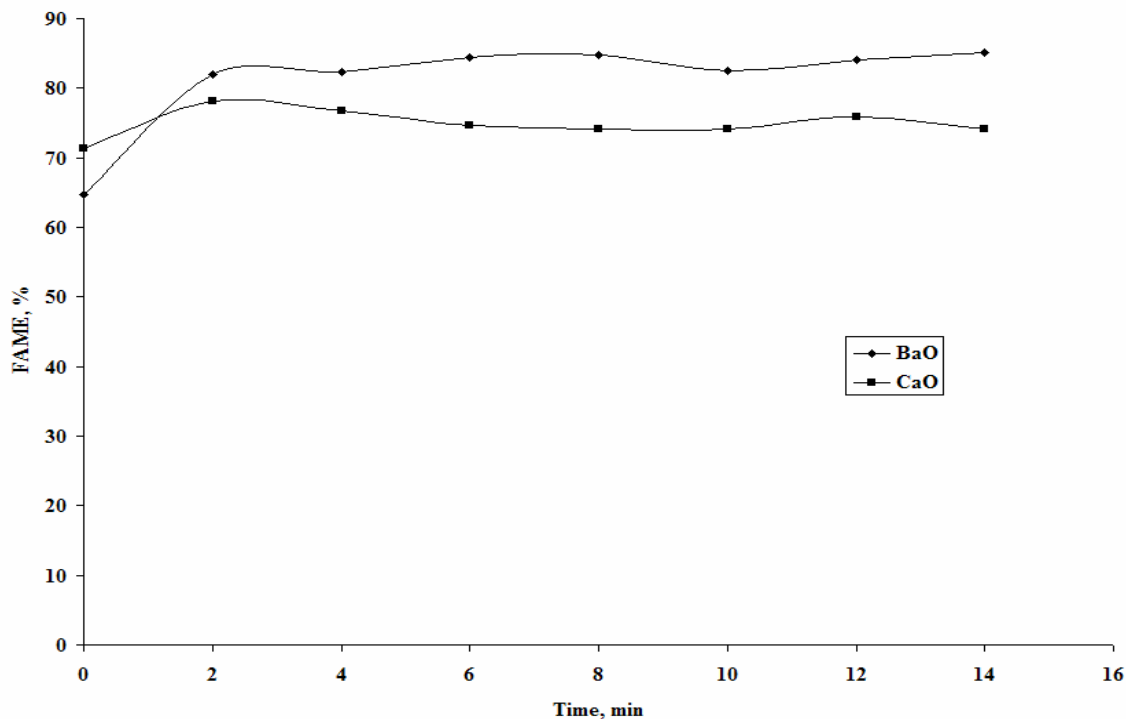


Figure 4.7 FAME yield for BaO and CaO (reaction times denoted represent time after reactants reached 215°C)

#### 4.2.2 Screening of mixed metal oxide

The prepared catalysts NaMO1, NaMO2, NaMO3 and NaMO4 were subjected to transesterification in a high pressure reactor for different temperatures and durations. 100 ml of soybean oil, 30 ml of methanol and 2 gm of each of catalysts were used for the transesterification at three different temperatures (70°C, 100°C and 215°C) in a high pressure reactor for 2 hrs. The sampling interval was 30 min. Finally, the percentages of fatty acid methyl esters (FAME) were evaluated using gas chromatography analysis. Figures 4.8, 4.9, 4.10 and 4.11 show the FAME yields with NaMO1, NaMO2, NaMO3 and NaMO4 respectively.

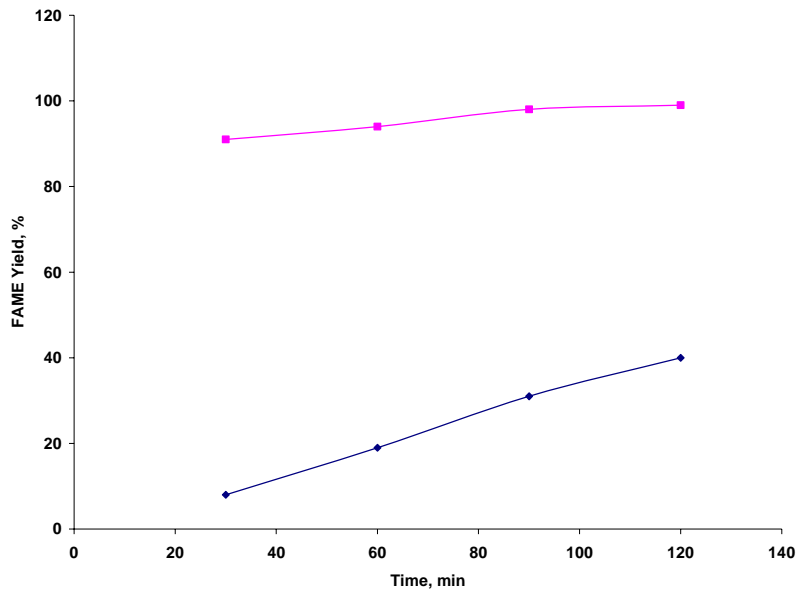


Figure 4.8 FAME yield for NaMO1 at two different temperatures

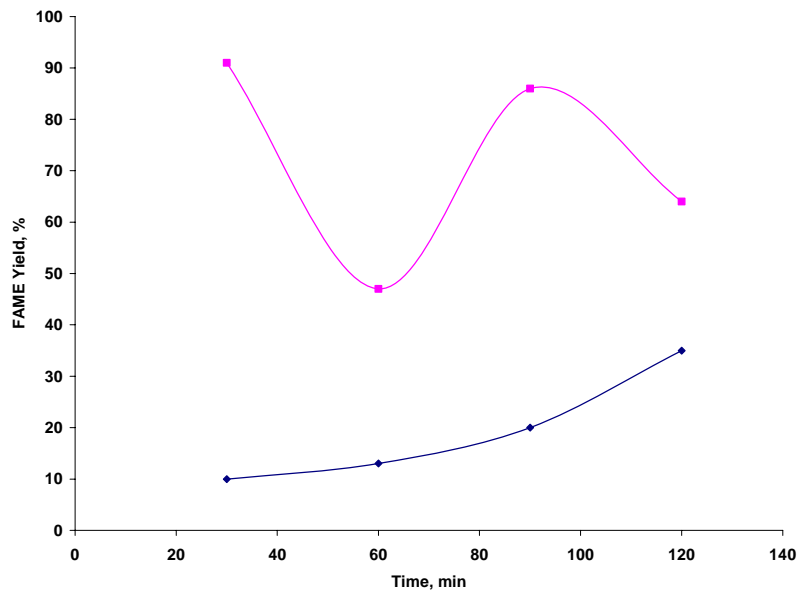


Figure 4.9 FAME yield for NaMO2 at two different temperatures

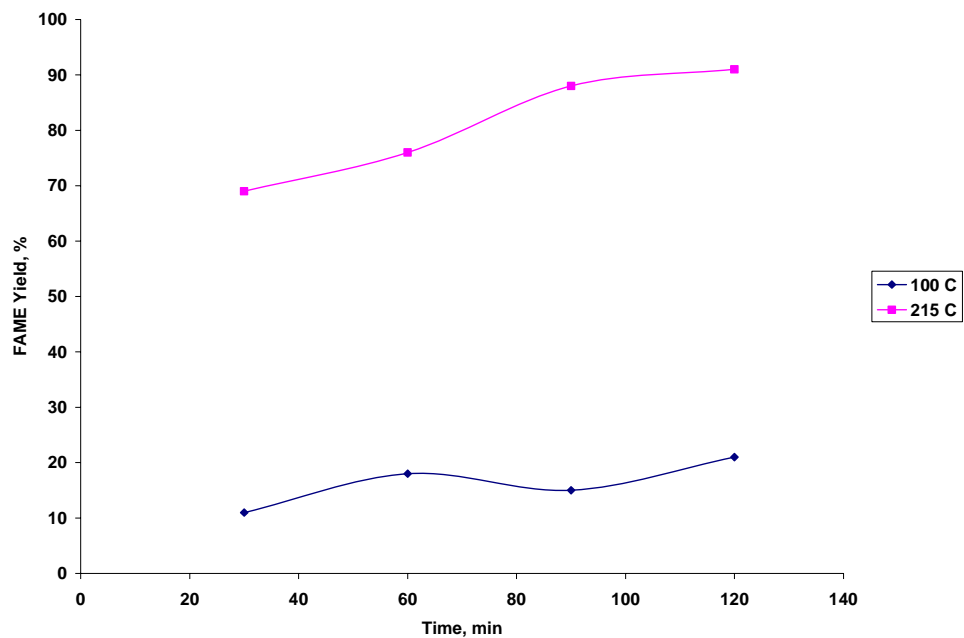


Figure 4.10 FAME yield for NaMO3 at two different temperatures

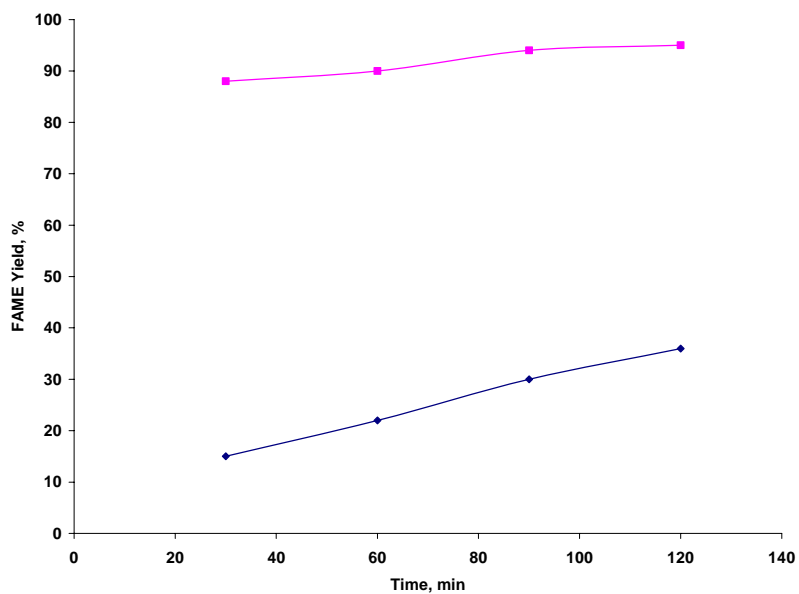


Figure 4.11 FAME yield for NaMO4 at two different temperatures



Among all four LDH catalysts tested, NaMO1 showed the highest yield, more than 99% selectivity towards the transesterification (Figure 4.8) at 215°C. Other catalysts also showed favorable transesterification yields. We reused the NaMO1 catalyst for the transesterification and it was found that more than 63% of the FAME was produced with the second use of the same NaMO1 catalyst.

#### 4.2.3 Screening of layered double hydroxides

Soybean oil, methanol and the prepared LDH catalysts were used for the transesterification at three different temperatures (65°C, 150°C and 215°C) in a high pressure reactor for three different time periods, i.e., 1, 2 and 4 hrs for two molar ratios of methanol and oil (15:1 and 40:1). Figure 4.12, 4.13 and 4.14 shows the FAME yield with LiLDH catalyst at three different reaction conditions.

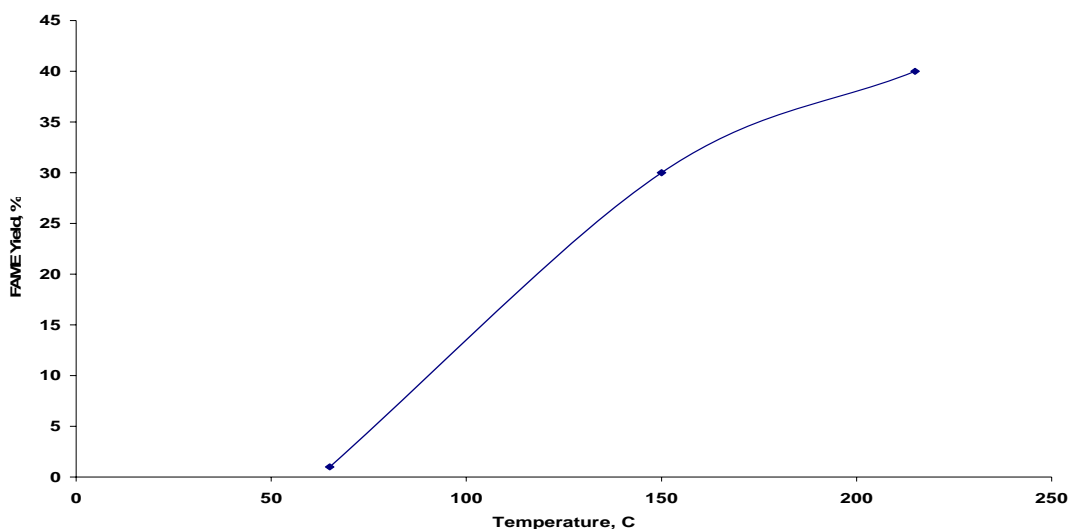


Figure 4.12 FAME yield with LiLDH at 15:1 methanol to oil ratio and 1 % (by wt.) of the catalyst for 1 hr of transesterification

It was observed that at 65°C, all reaction conditions yielded a very low amount of biodiesel. However, as the temperature increased there was an increase in FAME yield. The highest yield of 51 % was achieved at 15:1 methanol to oil ratio for 3 % of LiLDH after 4 h (Figure 4.14).

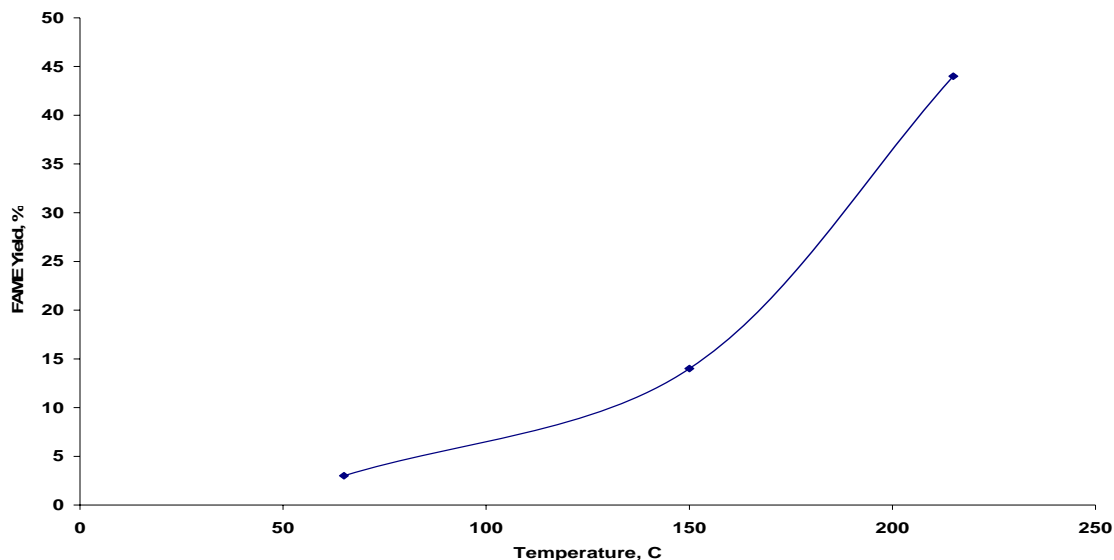


Figure 4.13 FAME yield with LiLDH at 40:1 methanol to oil ratio and 1 % (by wt.) of the catalyst for 2 hr of transesterification

It was observed that increasing the amount of catalyst resulted in higher FAME yields (Figure 4.14). However, increasing the amount of methanol did not result in better yields (Figure 4.12, 4.13). Although the amount of biodiesel produced with this particular catalyst was not too enticing, the results were encouraging due to the fact that it was proven that LDH is selective towards transesterification and since this is a true heterogeneous catalyst, LDH open a pathway to develop more robust heterogeneous catalysts.

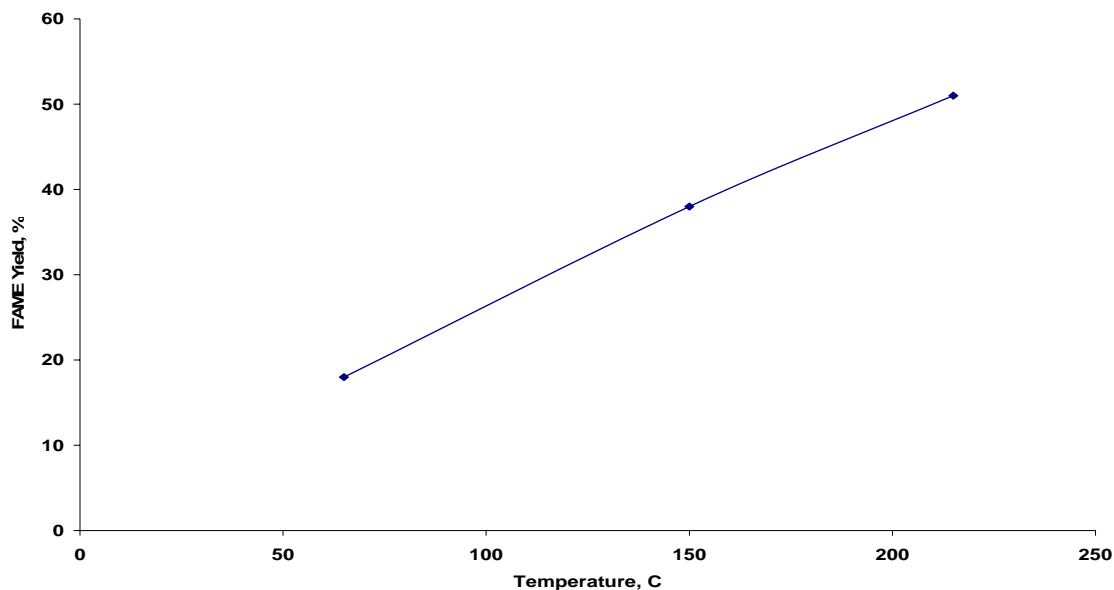


Figure 4.14 FAME yield with LiLDH at 15:1 methanol to oil ratio and 3 % (by wt.) of the catalyst for 4 hr of transesterification

### 4.3 Catalyst Characterization

#### 4.3.1 Surface area of the catalysts

Table 4.2 shows the surface area of the catalysts based on the nitrogen adsorption /desorption method (multipoint BET), and it was found that LiLDH had the largest area of 190.5 m<sup>2</sup>/g followed by MgO with 157.4 m<sup>2</sup>/g whereas the PbO<sub>2</sub> had the minimum of 0.38 m<sup>2</sup>/g. All the three lead catalyst were found to have a very small surface area (0.3-1.0 m<sup>2</sup>/g). All the NaMO catalysts showed approximately similar surface areas in the range of 7-14 m<sup>2</sup>/g, suggesting that different temperatures of catalysts preparation (25, 100, 150 and 200 °C) did not affect the surface area of the catalysts.

Table 4.2 Surface area of the metal oxides

| Catalyst                       | Surface area,<br>m <sup>2</sup> /g |
|--------------------------------|------------------------------------|
| PbO <sub>2</sub>               | 0.38                               |
| PbO                            | 0.55                               |
| BaO                            | 0.76                               |
| Pb <sub>3</sub> O <sub>4</sub> | 0.98                               |
| ZnO                            | 4.04                               |
| Tl <sub>2</sub> O <sub>3</sub> | 6.71                               |
| NaMO <sub>4</sub>              | 7.37                               |
| NaMO <sub>2</sub>              | 10.29                              |
| NaMO <sub>3</sub>              | 13.88                              |
| NaMO <sub>1</sub>              | 13.98                              |
| MnO <sub>2</sub>               | 50.55                              |
| CaO                            | 61.39                              |
| MgO                            | 157.4                              |
| LiLDH                          | 190.5                              |

#### 4.3.2 Acidity/ Basicity of the catalysts

Based on the methods described in the section 3.3.2 and 3.3.3 by using Hammett Indicators followed by the titration, acid/base site strength and acidity/basicity was determined. Table 4.3 shows the type of the catalyst with their site strength and acidity/basicity value. MgO was found to be highly basic with a basicity of 46.05 mmol of HCl / g of MgO and had a positive effect on the transesterification without cracking the methyl esters at the higher temperature. ZnO, PbO and PbO<sub>2</sub> was found to be

amphoteric with a site strength ( $H_{-}$ ) in the range of 6.8 and 8.2, and other than these three catalysts all the rest of the catalyst were found to be basic.

Table 4.3 Site strength of the metal oxides and their respective acidity/basicity value

| <b>Catalyst</b>                | <b>Type</b> | <b>Acid/ Base Site strength, (<math>H_{-}</math>)</b> | <b>Acidity, mmol of NaOH /g of catalyst</b> | <b>Basicity, mmol of HCl/g of catalyst</b> |
|--------------------------------|-------------|---|---|--|
| MgO                            | Basic       | 11<( $H_{-}$ )<15                                     |   | 46.05                                      |
| CaO                            | Basic       | 10.1<( $H_{-}$ )<11                                   |   | 16.24                                      |
| ZnO                            | Amphoteric  | 6.8<( $H_{-}$ )<8.2                                   | 12.25                                       | 32.35                                      |
| PbO                            | Amphoteric  | 6.8<( $H_{-}$ )<8.2                                   | 5.747                                       | 7.58                                       |
| PbO <sub>2</sub>               | Amphoteric  | 6.8<( $H_{-}$ )<8.2                                   | 17.86                                       | 7.00                                       |
| Pb <sub>3</sub> O <sub>4</sub> | Basic       | 6.8<( $H_{-}$ )<8.2                                   |   | 14.545                                     |
| Tl <sub>2</sub> O <sub>3</sub> | Basic       | 10.1<( $H_{-}$ )<11                                   |   | 15.93                                      |
| MnO <sub>2</sub>               | Basic       | 10.1<( $H_{-}$ )<11                                   |   | 16.53                                      |
| BaO                            | Basic       | 10.1<( $H_{-}$ )<11                                   |   | 21.21                                      |
| NaMO1                          | Basic       | 11<( $H_{-}$ )<15                                     |   | 9.86                                       |
| NaMO2                          | Basic       | 11<( $H_{-}$ )<15                                     |   | 9.8  |
| NaMO3                          | Basic       | 11<( $H_{-}$ )<15                                     |   | 7.814                                      |
| NaMO4                          | Basic       | 11<( $H_{-}$ )<15                                     |   | 7.81                                       |
| LiLDH                          | Basic       | 15<( $H_{-}$ )<18.2                                   |   | 21.2                                       |

As far as site strength was concern LiLDH shown a highest basic strength in the (H<sub>+</sub>) range of 15-18.2, followed by MgO and all the NaMO catalyst with a (H<sub>+</sub>) range of 11-15.

#### **4.3.3 Leaching analysis**

The leaching of the metal from the catalysts to the biodiesel and glycerol samples was analyzed by Flame Atomic Absorption Analysis (FLAA) in Mississippi State Chemical Laboratory, Mississippi State University. The technique of flame atomic absorption spectroscopy (FAAS) requires a liquid sample to be aspirated, aerosolized, and mixed with combustible gases, such as acetylene and air or acetylene and nitrous oxide. The mixture is ignited in a flame whose temperature ranges from 2100 to 2800 °C. During combustion, atoms of the element of interest in the sample are reduced to free, unexcited ground state atoms, which absorb light at characteristic wavelengths. The characteristic wavelengths are element specific and accurate to 0.01-0.1nm. Table 4.4 shows the amount of the metal leached in the biodiesel and glycerol sample.

Table 4.4 Leaching of metals from their respective metal oxide in biodiesel and glycerol sample

| <b>Catalyst</b>                | <b>Leaching in glycerol,<br/>mg/kg of Glycerol</b> | <b>Leaching in biodiesel,<br/>mg/kg of Biodiesel</b> |
|--------------------------------|--|--|
| PbO                            | 2100   | 13000  |
| ZnO                            | 45   | 110  |
| CaO                            | 1500   | 6800   |
| MgO                            | 460  | 8200   |
| PbO <sub>2</sub>               | 4400   | 710  |
| Tl <sub>2</sub> O <sub>3</sub> | 35000  | 19000  |
| Pb <sub>3</sub> O <sub>4</sub> | 8100   | 760  |

Thallium oxide had high leaching in both biodiesel and glycerol samples, whereas Zinc oxide had the minimum.

#### **4.3.4 X-Ray Diffractogram (XRD) and Scanning Electron Microscope (SEM) analysis**

Figure 4.15 shows scanning electron microscope (SEM) images of NaMO1, NaMO2, NaMO3 and NaMO4. The images depicts that the temperature has effect on their

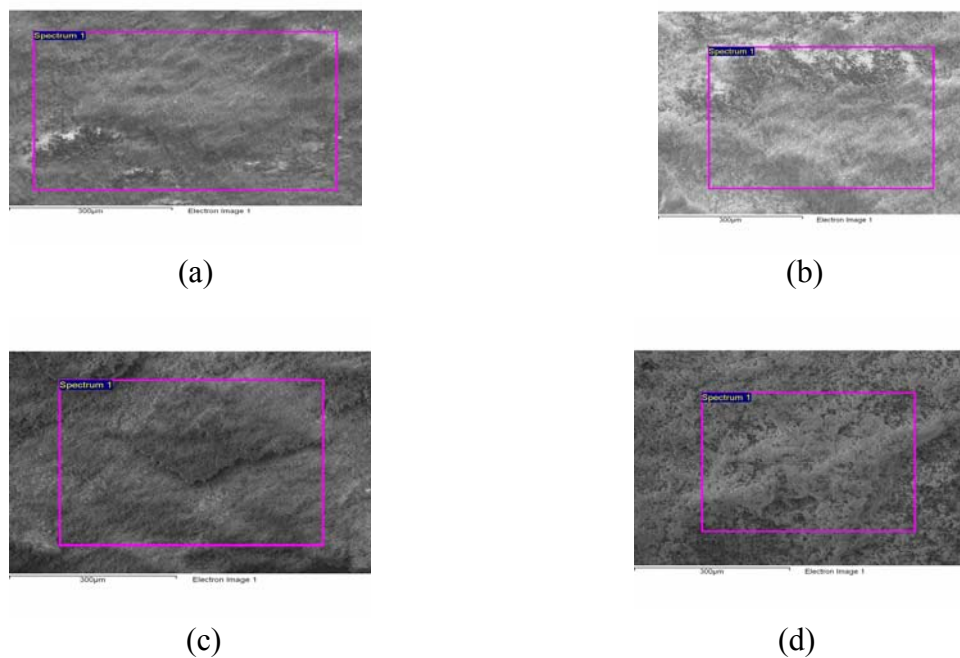


Figure 4.15 SEM images of (a)- NaMO1, (b)- NaMO2, (c)- NaMO3 and (d)- NaMO4

texture. It was found that the low temperature treatment showed highly dense and smooth characteristics. In this NaMO1 was found to be highly denser and smoother than other mixed oxide catalysts. Table 4.5 shows the elemental analysis of NaMO1, NaMO2, NaMO3 and NaMO4. It was found that NaMO has higher amount of Na (Sodium) in the catalyst, and this is the reason it has got the highest yield for transesterification.



Table 4.5 Elemental analysis of NaMO1, NaMO2, NaMO3 and NaMO4

| <b>Element</b> | <b>Weight%</b> | <b>Atomic%</b> |
|----------------|----------------|----------------|
| Na             | 11.23          | 29.67          |
| Si             | 28.53          | 56.58          |
| La             | 60.23          | 13.75          |
| Totals         | 100.00         |                |

(a)- NaMO1

| <b>Element</b> | <b>Weight%</b> | <b>Atomic%</b> |
|----------------|----------------|----------------|
| Na             | 10.38          | 26.84          |
| Si             | 28.94          | 56.16          |
| Al             | 2.48           | 2.86           |
| La             | 56.92          | 12.72          |
| Totals         | 100.00         |                |

(b)- NaMO2

| <b>Element</b> | <b>Weight%</b> | <b>Atomic%</b> |
|----------------|----------------|----------------|
| Na             | 3.13           | 10.52          |
| Si             | 27.45          | 69.30          |
| La             | 69.42          | 20.18          |
| Totals         | 100.00         |                |

(c)- NaMO3

| <b>Element</b> | <b>Weight%</b> | <b>Atomic%</b> |
|----------------|----------------|----------------|
| Na             | 3.52           | 10.90          |
| Si             | 26.57          | 61.79          |
| Al             | 3.77           | 5.20           |
| La             | 61.98          | 16.60          |
| Totals         | 100.00         |                |

(d)- NaMO4

Figure 4.16 to 4.19 shows the X-ray diffractogram patterns for NaMO1, NaMO2, NaMO3 and NaMO4 respectively, and it can be shown that all the NaMO catalysts follows the same spectrum.

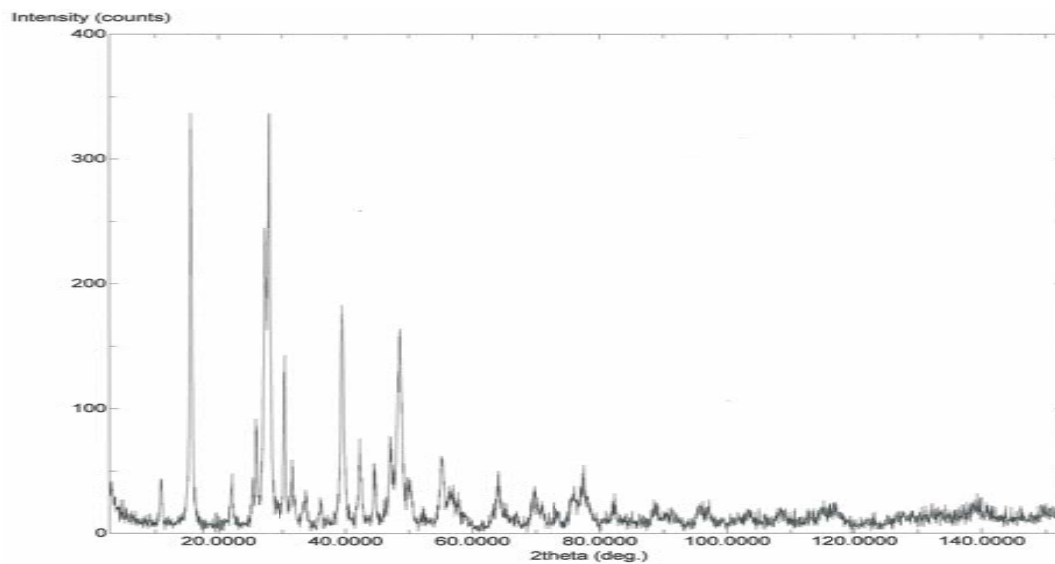


Figure 4.16 X-ray patterns for NaMO1

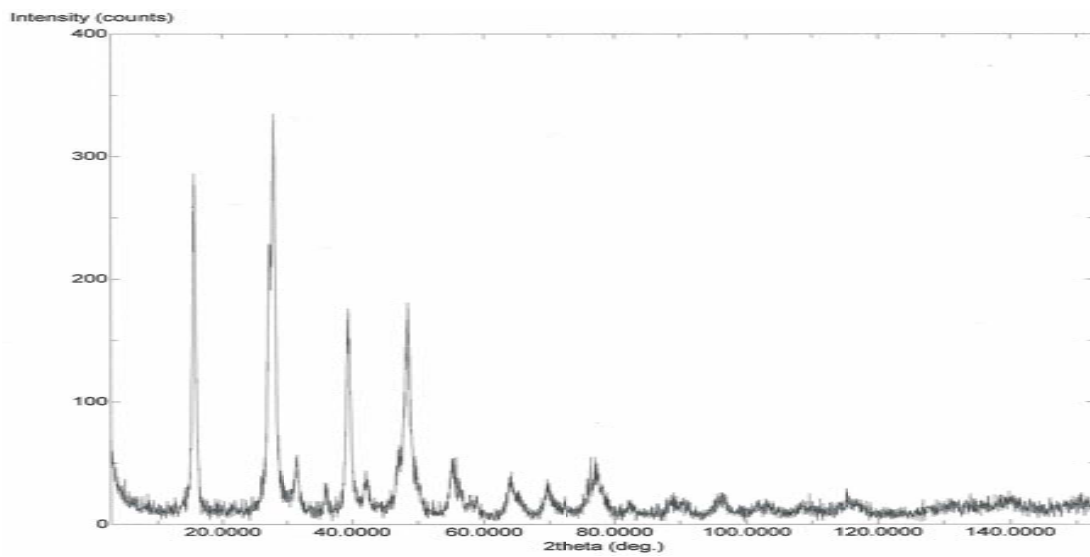


Figure 4.17 X-ray patterns for NaMO<sub>2</sub>

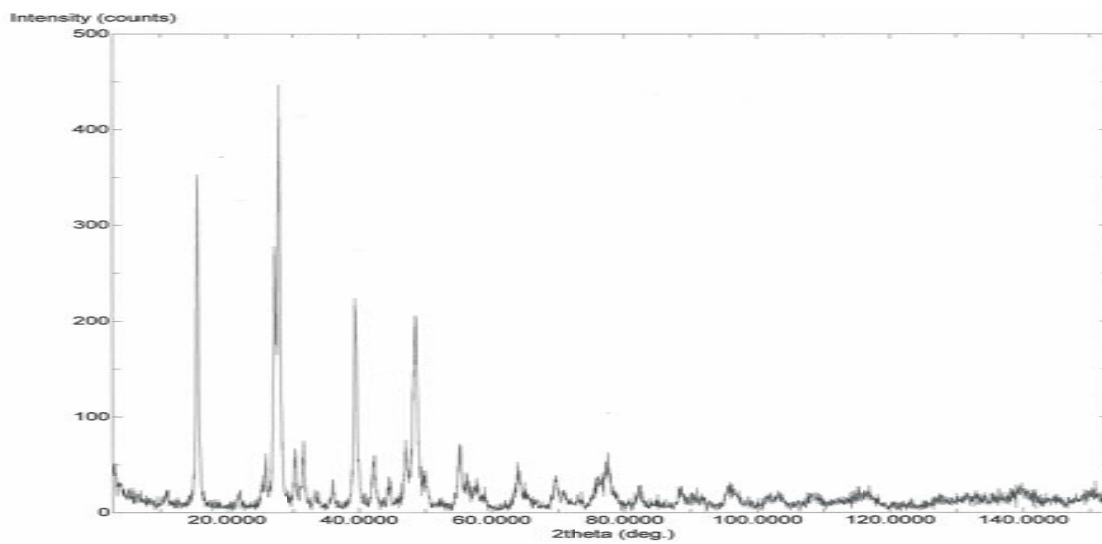


Figure 4.18 X-ray patterns for NaMO<sub>3</sub>

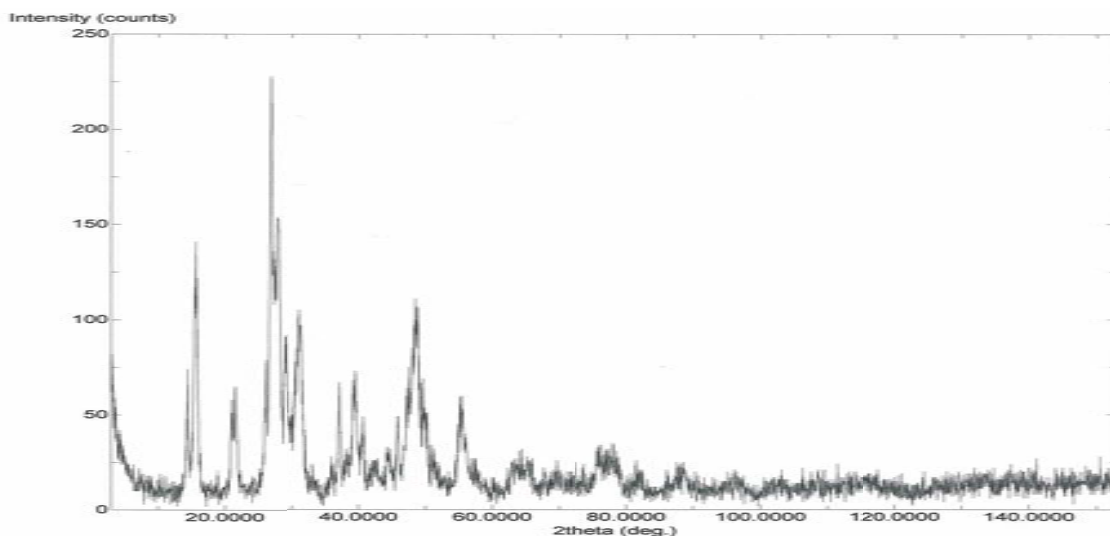


Figure 4.19 X-ray patterns for NaMO4

#### 4.4 Reaction Kinetics Determination

Based on the principles discussed in Section 3.4, all eight cases for each catalyst were plotted and the coefficient of correlation ( $R^2$ ) was determined for each case. Finally the case with the highest coefficient of correlation ( $R^2$ ) was selected for the determination of rate constant and reaction order. Table 4.6 gives the  $R^2$  values of all eight cases for each of the 5 catalysts.

For some experimental units, Table 4.6 renders an array of  $R^2$  values because the data has been transferred in the form of  $y=mx$  in order to model the reaction order based on Equation 3.7 to 3.14. For each catalyst, the highest  $R^2$  value is selected out of the 8 cases and the corresponding values of slope (the rate constant, as discussed in section 3.4) were determined. Table 4.7 gives the reaction order of the transesterification w.r.t., each of the reactants, as well as the overall reaction order and the value of rate constant for each of the catalysts. It was observed that as the rate constant per unit surface area of the

catalyst increases the FAME yield increases. However we did not use all NaMO catalysts, because it was found that they are almost similar in their properties and structure. So we just used NaMO1 (High yield catalyst) for the kinetics determination.

Table 4.6 The value of coefficient of determination ( $R^2$ ) of all eight cases for each catalyst

| <b>Catalysts →<br/>Cases<br/>↓</b> | <b>PbO</b> | <b>MgO</b> | <b>MnO<sub>2</sub></b> | <b>BaO</b> | <b>CaO</b> | <b>NaMO1</b> |
|------------------------------------|------------|------------|------------------------|------------|------------|--------------|
| 1                                  | 0.90       | 0.91       | 0.87                   | 0.39       | 0.48       | 0.40         |
| 2                                  | 0.89       | 0.90       | 0.85                   | 0.49       | 0.45       | 0.89         |
| 3                                  | 0.91       | 0.93       | 0.88                   | 0.41       | 0.49       | 0.41         |
| 4                                  | 0.88       | 0.88       | 0.83                   | 0.51       | 0.44       | 0.94         |
| 5                                  | 0.83       | 0.83       | 0.77                   | 0.61       | 0.41       | 0.75         |
| 6                                  | 0.90       | 0.91       | 0.86                   | 0.42       | 0.46       | 0.40         |
| 7                                  | 0.81       | 0.80       | 0.74                   | 0.63       | 0.41       | 0.74         |
| 8                                  | 0.86       | 0.85       | 0.80                   | 0.53       | 0.44       | 0.97         |

Table 4.7 Reaction order of the transesterification w.r.t. each of the reactant as well as overall and the rate constant

| Catalyst         | Order w.r.t. Triglyceride | Order w.r.t. Methanol | Overall Order | Rate Constant  |
|------------------|---------------------------|-----------------------|---------------|--|
| PbO              | 0                         | 1                     | 1             | 0.0058, min <sup>-1</sup> m <sup>-2</sup>                                  |
| MgO              | 0                         | 1                     | 1             | 0.000007, min <sup>-1</sup> m <sup>-2</sup>                                |
| MnO <sub>2</sub> | 0                         | 1                     | 1             | 0.00003, min <sup>-1</sup> m <sup>-2</sup>                                 |
| BaO              | 2                         | 1                     | 3             | 0.011, m <sup>6</sup> mole <sup>-2</sup> min <sup>-1</sup> m <sup>-2</sup> |
| CaO              | 0                         | 1                     | 1             | 0.000008, min <sup>-1</sup> m <sup>-2</sup>                                |
| NaMO1            | 1                         | 2                     | 3             | 429, m <sup>6</sup> mole <sup>-2</sup> min <sup>-1</sup> m <sup>-2</sup>   |

#### 4.5 Reactor Modeling

Based on the high yield catalyst (NaMO1) from the screening analysis, we model batch reactor. We also did some more kinetics analysis for NaMO1 in terms of activation energy ( $E_a$ ) and pre-exponential factor (A) which was needed for the reactor modeling in Arrhenius equation. Equation 4.1 shows the Arrhenius equation.

$$k = A \exp^{-\frac{E_a}{RT}} \quad (4.1)$$

Where,

K is the rate constant

A is the pre exponential factor

$E_a$  is the activation energy

R is the universal gas constant

T is the absolute temperature

Based on the principles discussed in Section 3.4, we evaluated the rate constant for NaMO1 at two different temperatures. Table 4.8 shows the value of rate constant, activation energy and pre-exponential factor for NaMO1.

Table 4.8 Activation energy and pre-exponential factor data for NaMO1

| <b>Temperature,</b><br><b>(°C)</b> | <b>Rate Constant,</b><br><b>(m<sup>6</sup>mole<sup>-2</sup>min<sup>-1</sup>g<sup>-1</sup>)</b> | <b>Activation</b><br><b>Energy,</b><br><b>(Joulemole<sup>-1</sup>)</b> | <b>Pre-exponential Factor</b> |
|------------------------------------|--|--|-------------------------------|
| 100                                | 197.8  | 4.441 x10 <sup>4</sup>   | 4.939 x 10 <sup>6</sup>       |
| 215                                | 5581.6   |  |                               |

A batch reactor (liquid) with constant volume was modeled in the study.

Theoretically in a batch reactor, no mass enters or leave the system. The species mass balance is given by equation 4.2:

$$\frac{d(c_i V_r)}{dt} = V_r r_i \quad (4.2)$$

This takes into account the effect of changing volume. In equation 4.2,  $c_i$  is the species molar concentration (mol/m<sup>3</sup>),  $V_r$  denotes the reactor volume (m<sup>3</sup>), and  $r_i$  is the species rate expression (mol/m<sup>3</sup>.min.g) for solid catalysis. For an incompressible and ideally mixed reacting liquid, the energy balance at constant temperature is:

$$V_r \sum_i c_i C_{p,i} \frac{dT}{dt} = 0 \quad (4.3)$$

In the equation 4.3  $C_{p,i}$  is the species molar heat capacity (J/mol.K),  $T$  is the temperature (K), and  $t$  is the time (min). Since the temperature is constant the right hand term is equal to zero. The heat of the reaction can be written as

$$Q = -V_r \sum_j H_j r_j \quad (4.4)$$

Where  $H_j$  is the enthalpy of reaction (J/mol.K), and  $r_j$  is the reaction rate (mol/m<sup>3</sup>.min.g). For the reactor modeling analysis, we used methyl linoleate because almost 60% of soybean oil consists of methyl linoleate. All the thermodynamic data were obtained from Yaws (1999) for example the data for  $C_p$ ,  $H$  (enthalpy). The rate expression used in this study is given in equation 4.5.

$$r_j = k C_{TG} C_{ME}^2 \quad (4.5)$$

Where  $C_{TG}$  and  $C_{ME}$  were the concentrations of methyl linoleate and methanol respectively.

The variables changed in the modeling were the temperature and oil to methanol ratio. Three different temperature of 115, 215 and 315 °C were used whereas for the oil to methanol ratio three different ratio of 1:3, 1:6 and 1:9 were used. Figure 4.20 to 4.22 shows the concentration profile of Linoleic acid(TG), methyl linoleate(BD) and methanol(ME) at 115, 215 and 315°C for 1:6 oil to methanol ratio. Figure 4.23 to 4.25 shows the concentration profile of Linoleic acid, methyl linoleate and methanol at 1:3, 1:6 and 1:9 oil to methanol ratio at 215°C. As it can be seen from the figure 4.20 to 4.22, as the temperature increased the system reached equilibrium conditions fast. The situation



was similar with oil to methanol ratio - as the ratio increased the reaction reached its equilibrium fast. Figure 4.26 shows the Comparison of experimental and the model reaction rate at 215°C w.r.t. time using rate model with NaMO1, and it can be seen that the predicted model fits to the experimental data. The slight disparity could be attributed to 1). The model makes predictions based on ideal conditions and therefore, the predicted concentration was maximum for any given condition and 2). The model was based on methyl linoleate while the actual products from soybean oil ranges from C16 - C 18 FAMES.

## **4.6 Biodiesel Upgrading**

### **4.6.1 Mass spectrometer results**

As described in Section 3.5.2, we used two different experimental methods in order to upgrade the biodiesel. In the first experiment methyl linoleate was used for the analysis and the catalyst used were  $\text{MoO}_2\text{Cl}_2$  (5% mol) in dry toluene (5 ml) and Phenyl Silane ( $\text{PhSiH}_3$ ) (2.0 mmol) under nitrogen atmosphere. After the reaction mixture was stirred at reflux temperature of 115°C for 20 h, the mass spectrometric analysis did not indicate any deoxygenation and at the same time it was not economically feasible because of longer period of reaction. However we were able to remove one double bond from the methyl linoleate and were able to produce 10-Octadecenoic acid methyl ester (with 90% probability) . Although the treatment increased the oxidative stability of the methyl ester by removing unsaturation, the results were not that convincing because our

objective was to deoxygenate the ester. Hence we went for a second alternative treatment where biodiesel was treated with HZSM-5 in an attempt to deoxygenate.

In the second experiment, we used biodiesel with HZSM-5 zeolite (Calcined ZSM at 450°C for 4 hrs). The deoxygenation was done using 100 ml of pure biodiesel was mixed with 2 g of HZSM-5 catalyst in a high pressure reactor (Parr reactor) at three different temperatures of 215, 315 and 375°C for 10 hrs.

The results of the mass spectrometric analysis indicated several deoxygenated products in the form of aliphatic and aromatic hydrocarbons and with higher probability (more than 90 %). The compounds detected were xylene, 1, 2, 3-trimethyl benzene, 1, 2, 3, 4 -tetramethyl benzene, 9-octadecyne, tetradecane, pentadecane hexadecane, nonadecane and some lower molecular weight methyl esters. Also the three different temperatures had significant effect on deoxygenation. Figures 4.27, 4.28 and 4.29 shows the product spectrum at 215, 315 and 375 °C. It can be seen that at 375 °C (Figure 4.29) there were larger numbers of deoxygenated hydrocarbons. This was a qualitative analysis for the biodiesel upgrading. Section 4.6.2 will deal with the approximate quantitative analysis (thermodynamic analysis) at equilibrium conditions.



Figure 4.20 Conversion of Linoleic acid to methyl linoleate at 115°C and 1:6 oil to methanol ratio w.r.t. time with NaMOI



Figure 4.21 Conversion of Linoleic acid to methyl linoleate at 215°C and 1:6 oil to methanol ratio w.r.t. time with NaMOI

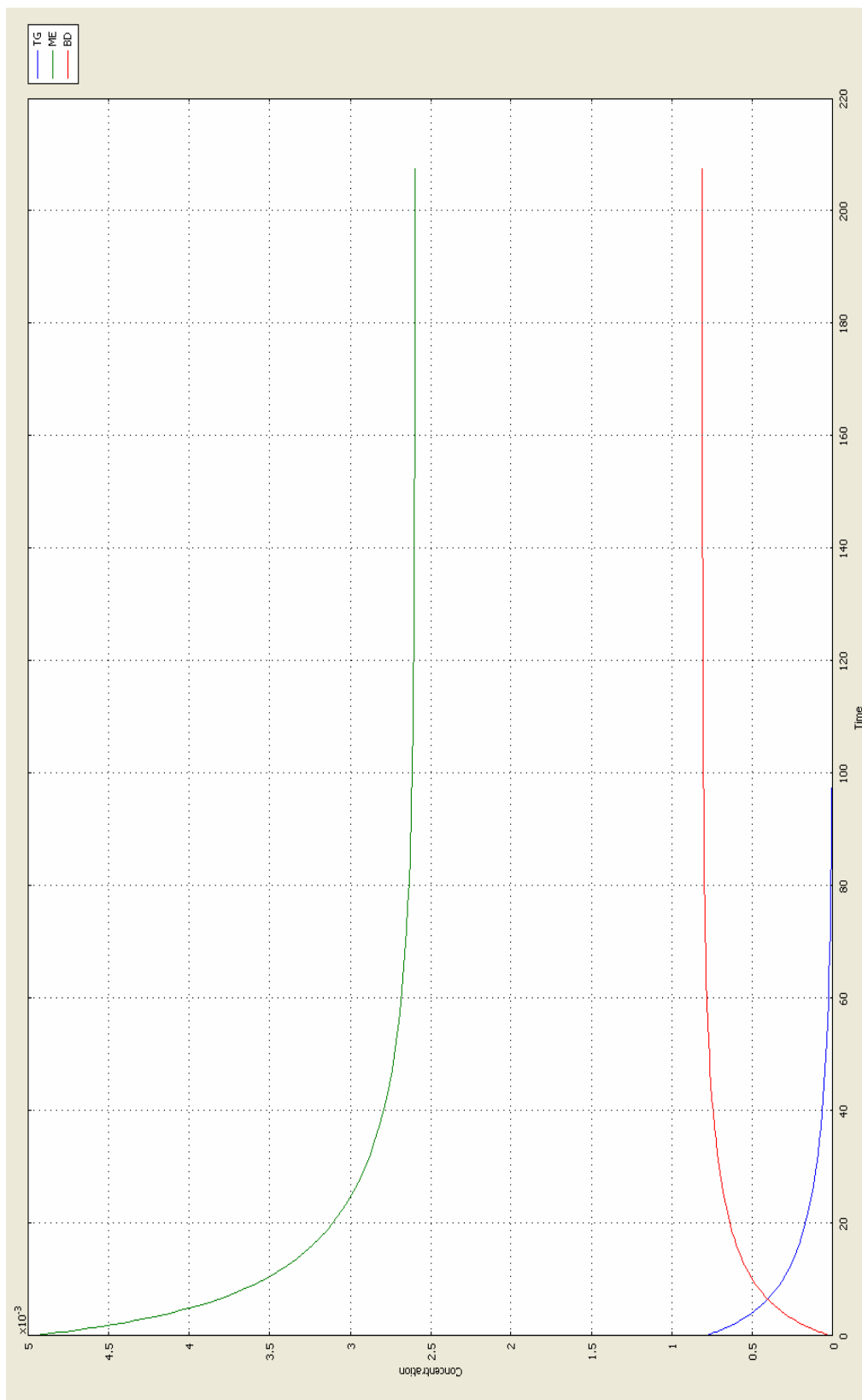


Figure 4.22 Conversion of Linoleic acid to methyl linoleate at 315°C and 1:6 oil to methanol ratio w.r.t. time with NaMOI

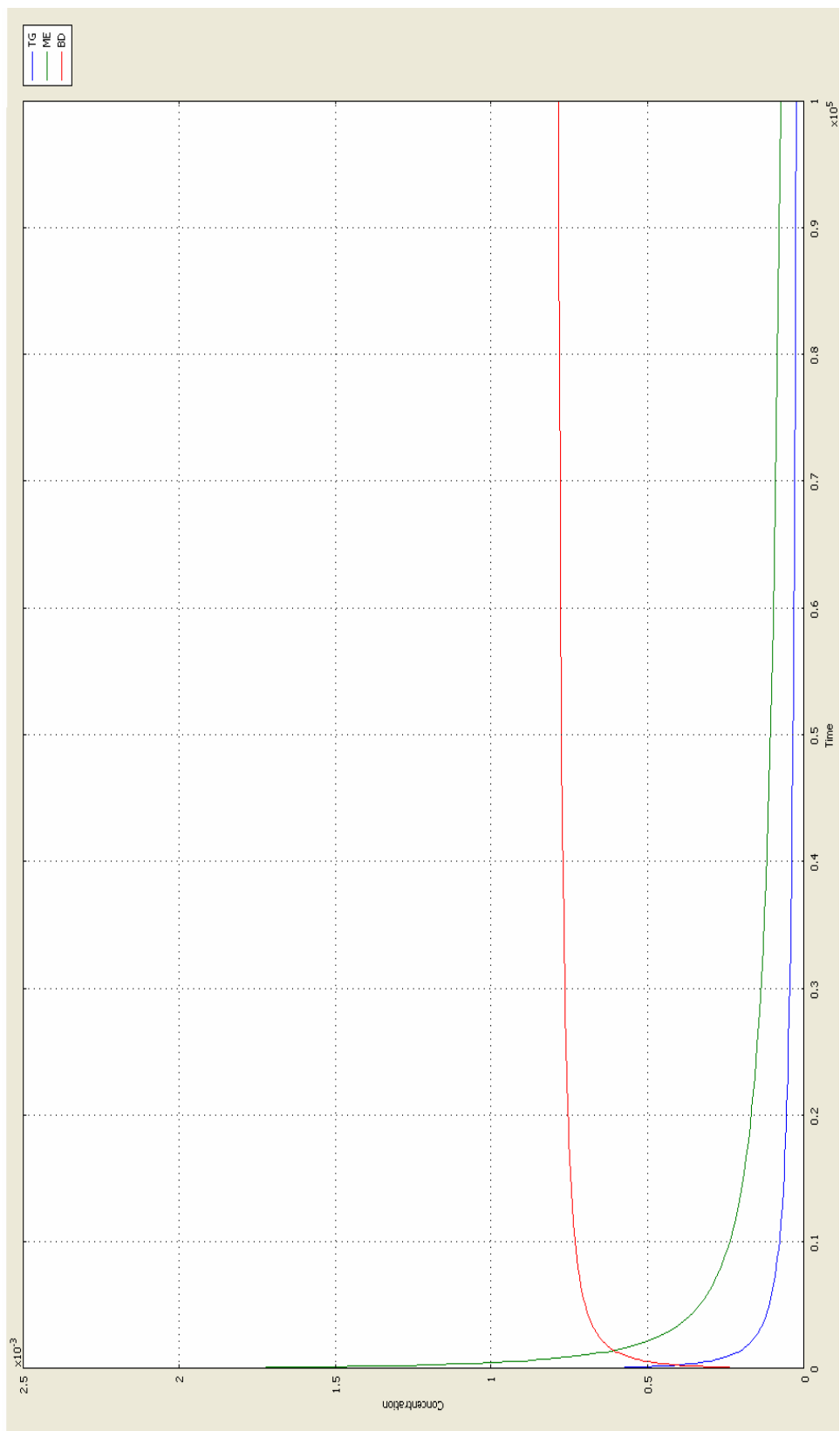


Figure 4.23 Conversion of Linoleic acid to methyl linoleate at 215°C and 1:3 oil to methanol ratio w.r.t. time with NaMOI

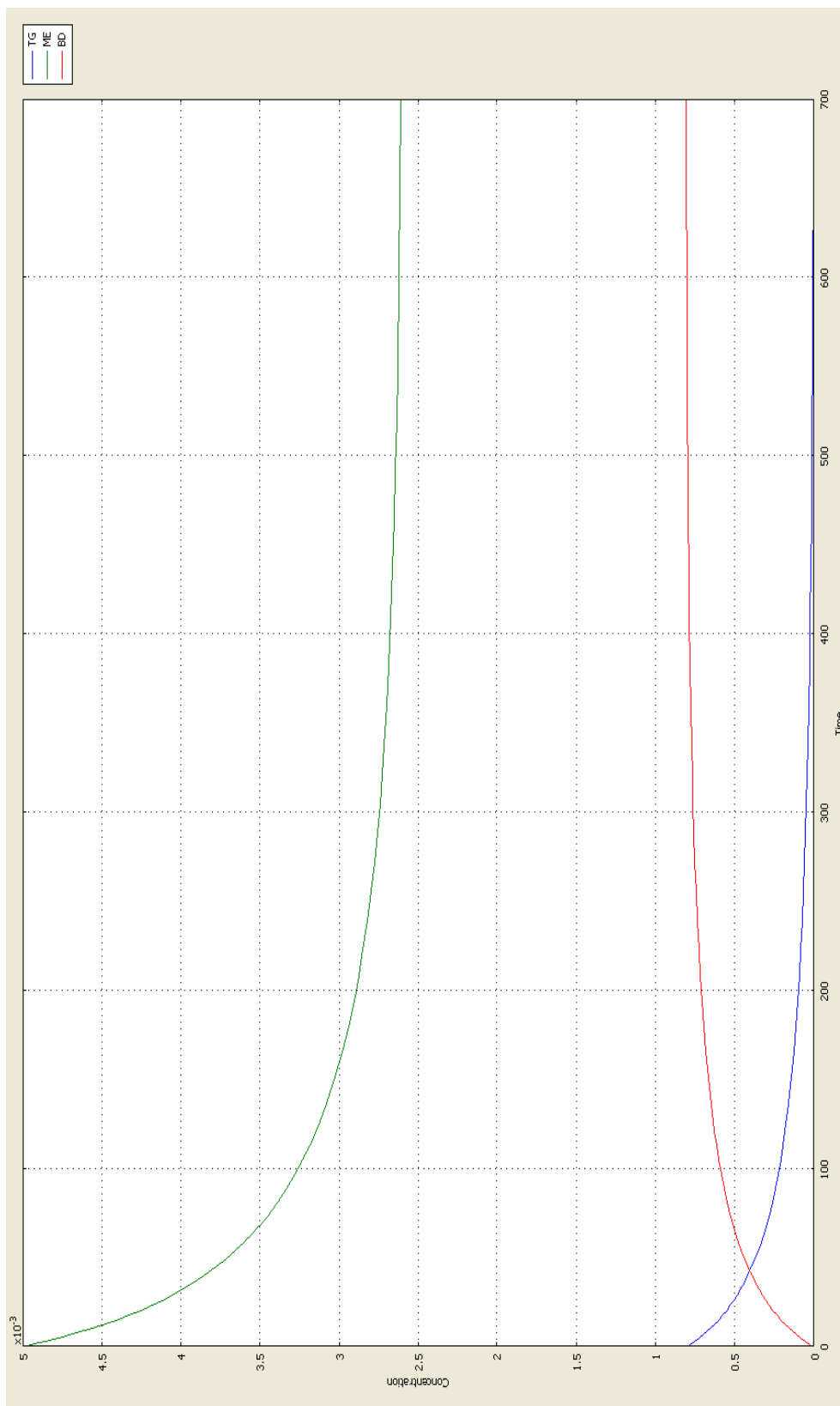


Figure 4.24 Conversion of Linoleic acid to methyl linoleate at 215°C and 1:6 oil to methanol ratio w.r.t. time with NaMOI

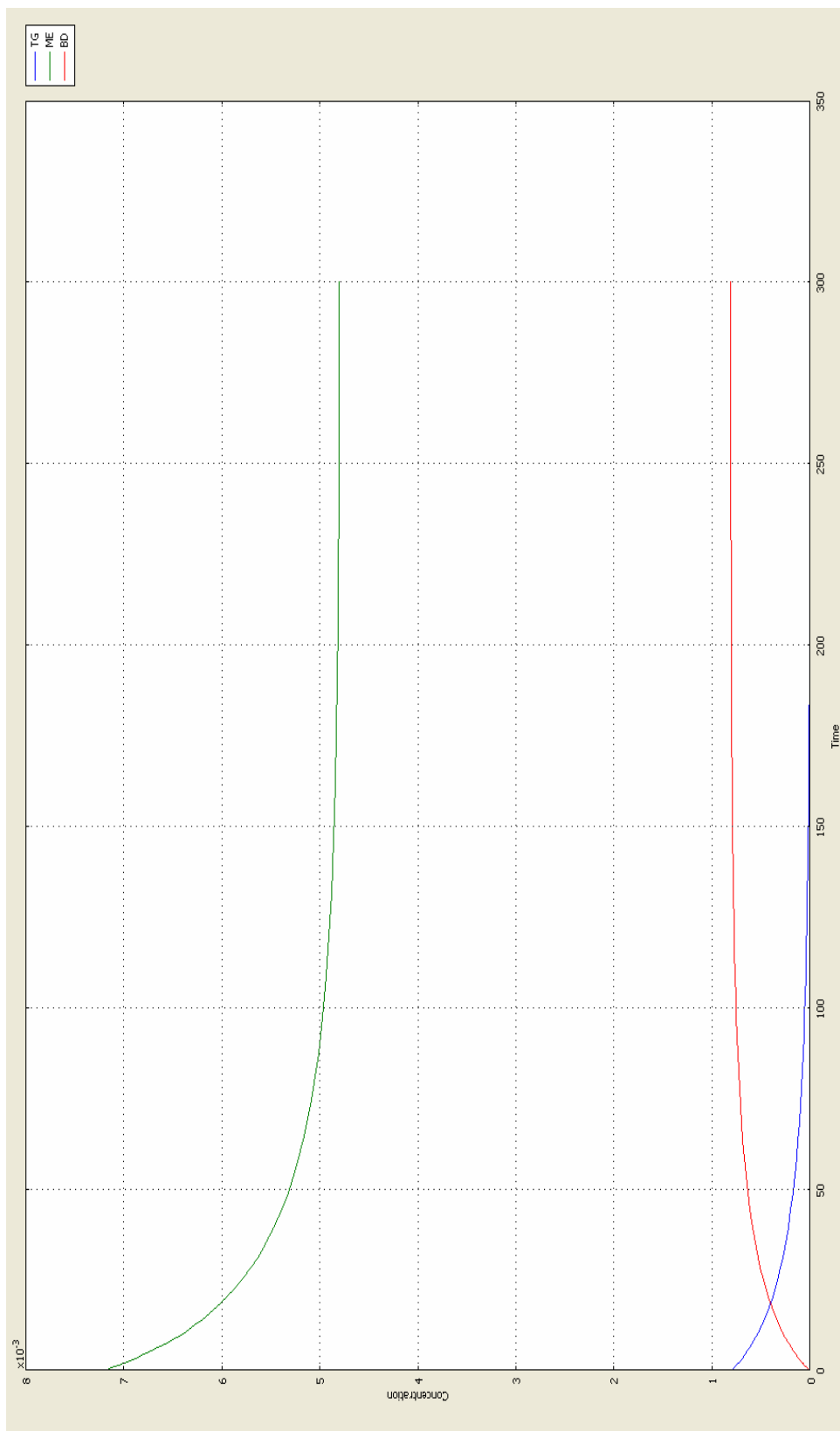


Figure 4.25 Conversion of Linoleic acid to methyl linoleate at 215°C and 1:9 oil to methanol ratio w.r.t. time with NaMOI



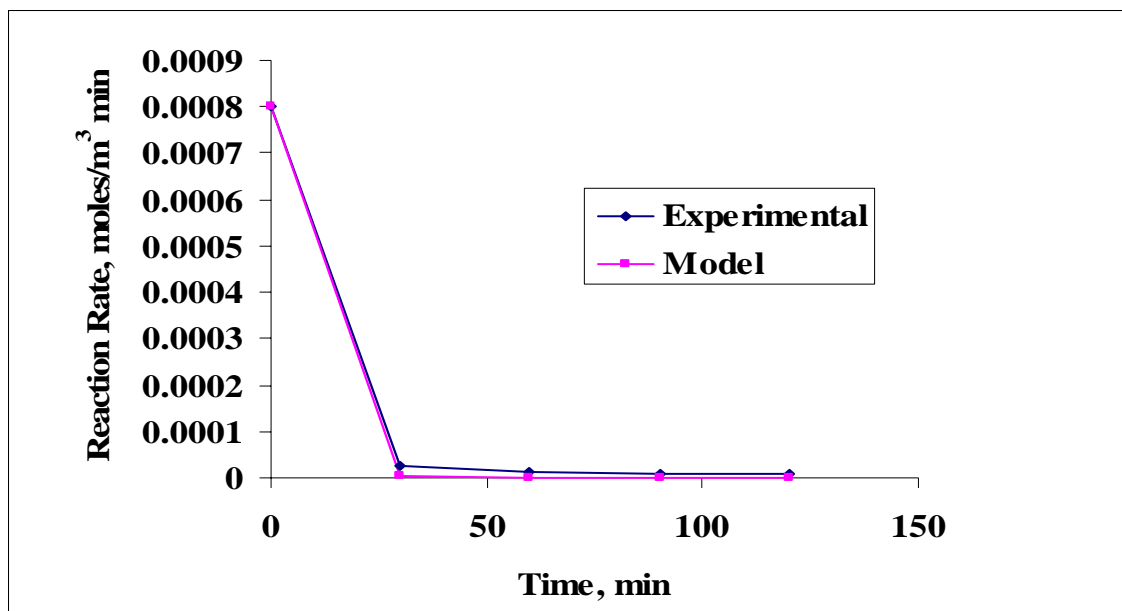
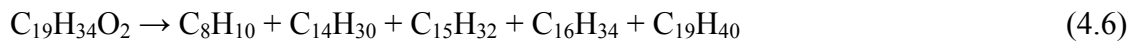


Figure 4.26 Comparison of experimental and the model reaction rate at 215°C w.r.t. time using rate model with NaMO1

#### 4.6.2 Thermodynamic analysis of methyl linoleate

We did a thermodynamic analysis for methyl linoleate. Based on the results from the mass spectrometric qualitative analysis, we were able to detect some deoxygenated product like xylene, nanodecane, hexadecane, pentadecane and tetradecane. Equation 4.6 shows the general expression of deoxygenation reaction of methyl linoleate.



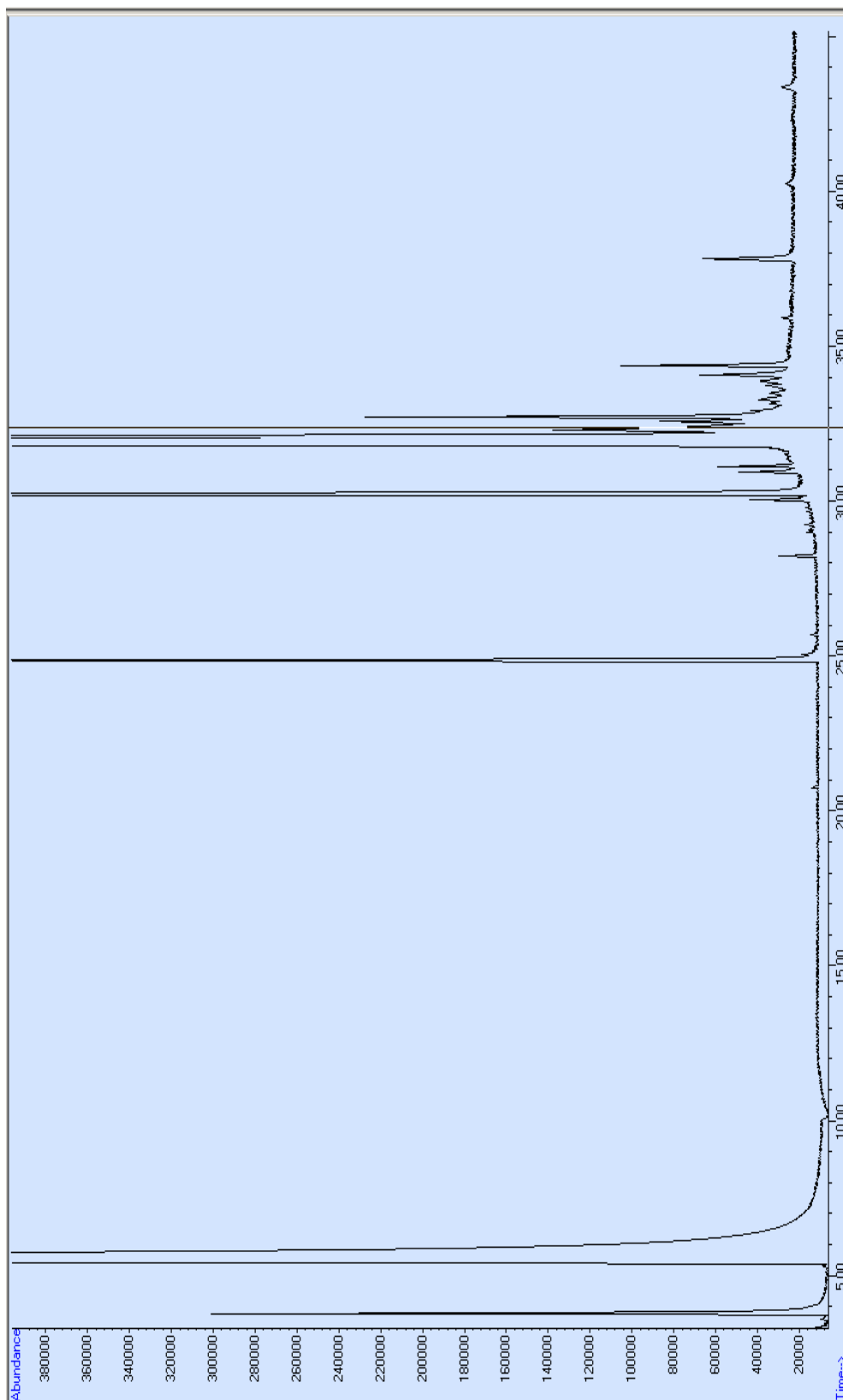


Figure 4.27 Spectrum of deoxygenation of biodiesel with HZSM-5 at 215 °C

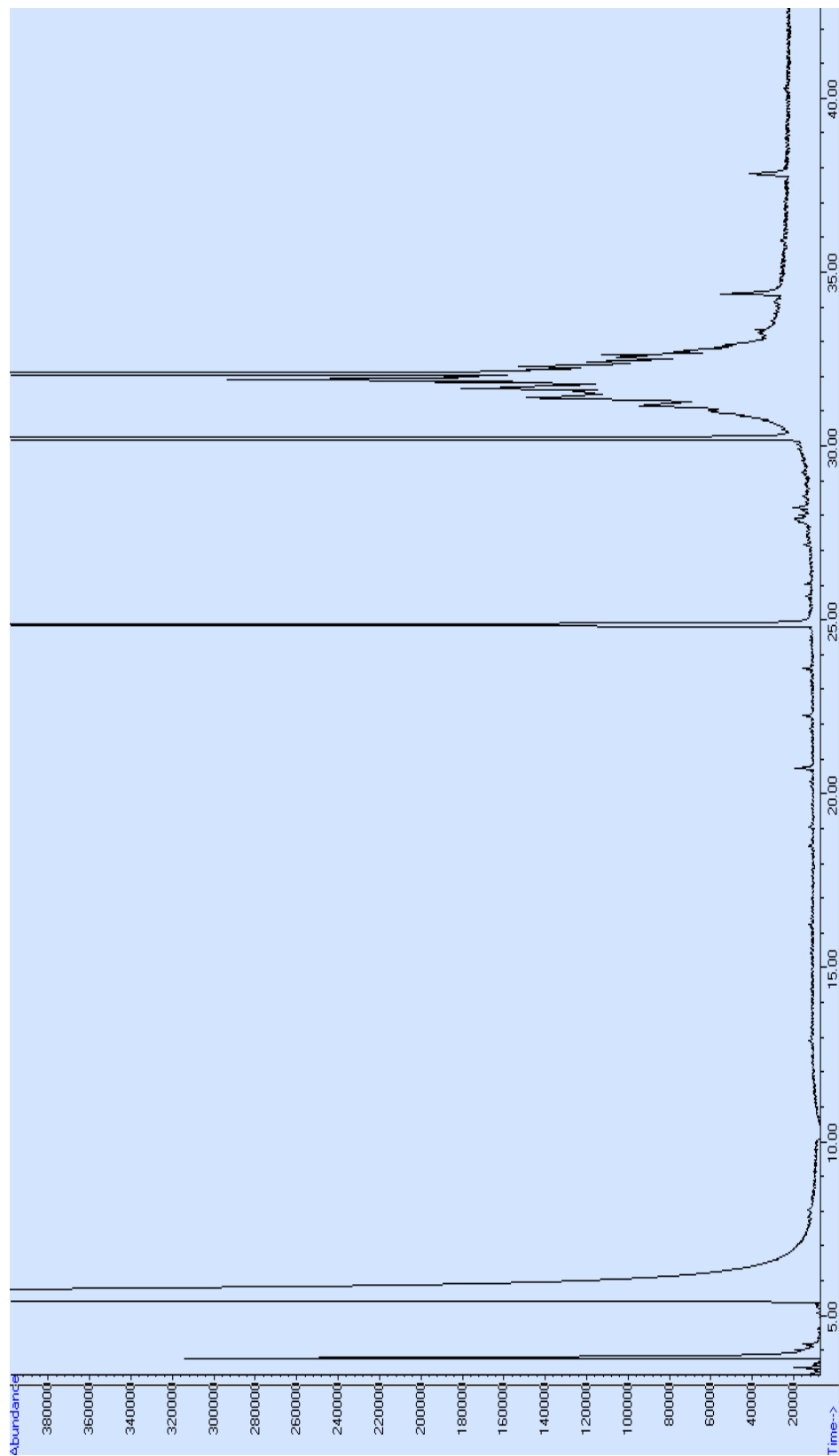


Figure 4.28 Spectrum of deoxygenation of biodiesel with HZSM-5 at 315 °C

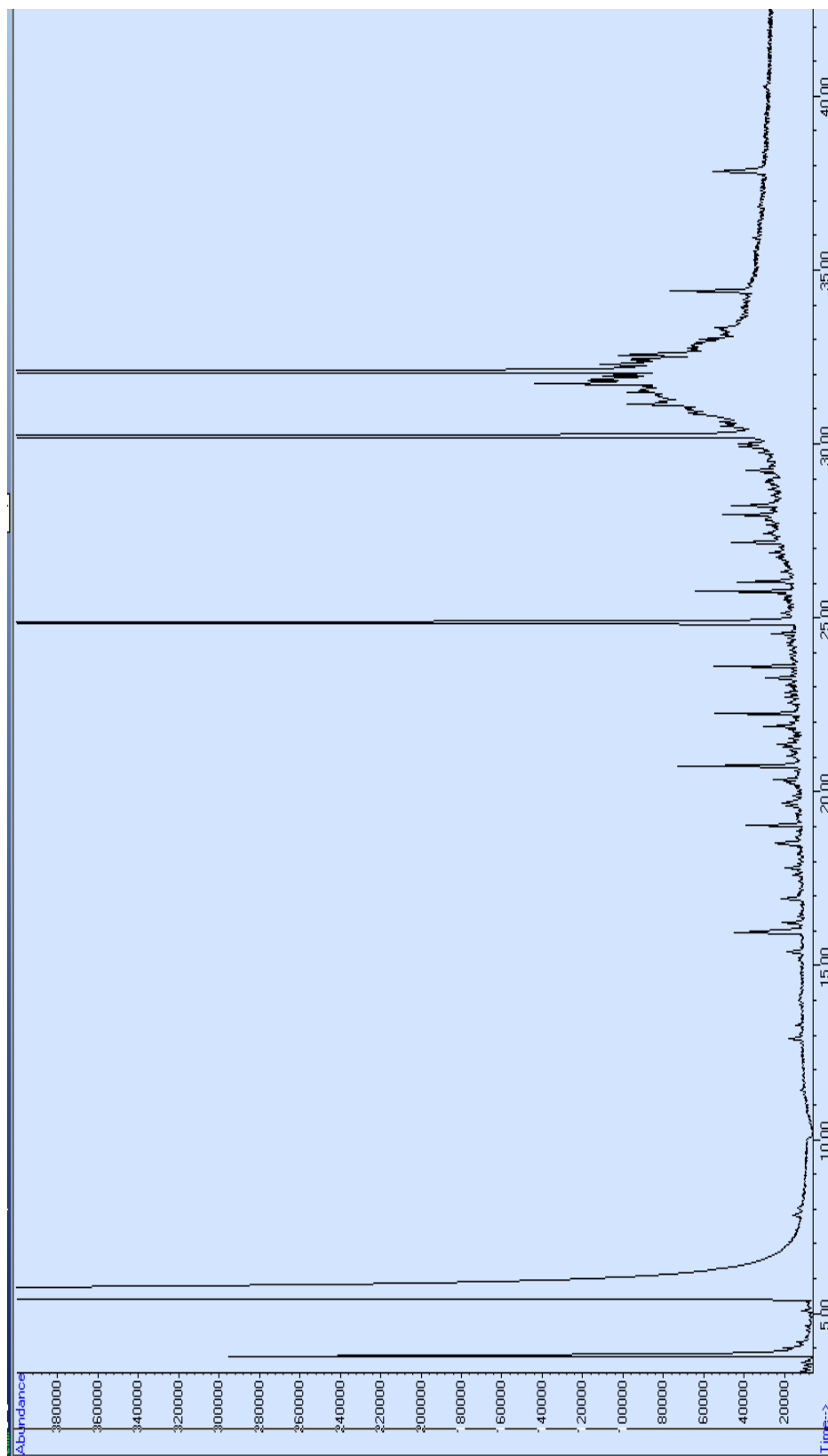


Figure 4.29 Spectrum of deoxygenation of biodiesel with HZSM-5 at 375 °C

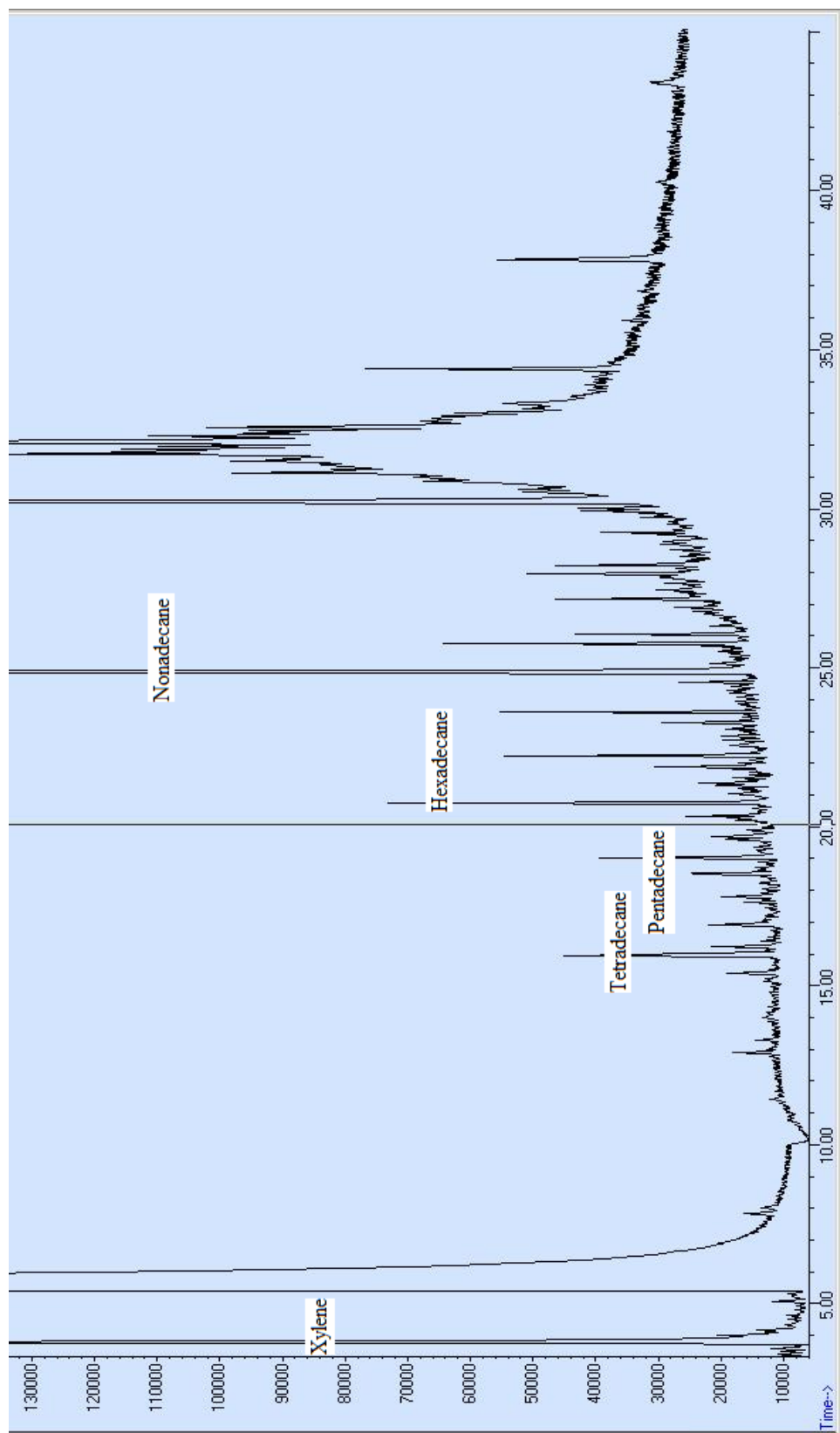


Figure 4.30 Detected peaks of deoxygenated compounds on the mass spectrometer

Constraints for the Mixture:

- The number of moles must be positive:

$$n_i > 0, \quad i=1, 2, 3, 4, 5$$

- There are 3 mass balance relationships,

$$19 = 8 * n_1 + 14 * n_2 + 15 * n_3 + 16 * n_4 + 19 * n_5$$

$$34 = 10 * n_1 + 30 * n_2 + 32 * n_3 + 34 * n_4 + 40 * n_5$$

$$2 = 0$$

Where,

$n_1$  is xylene

$n_2$  is tetradecane

$n_3$  is pentadecane

$n_4$  is hexadecane

$n_5$  is nonadecane

Figure 4.31 shows the result of the thermodynamic analysis, as it can be seen that the amount (number of moles) of xylene, tetradecane and pentadecane was higher than hexadecane and nonadecane. However, the difference in the number of moles of the spectrum of compounds is not that significant over the temperatures range of 100 – 600°C. According to Figure 4.30, we can expect that thermodynamically, a maximum of 0.93 moles of xylene, 0.52 moles of tetradecane, 0.19 moles of pentadecane and

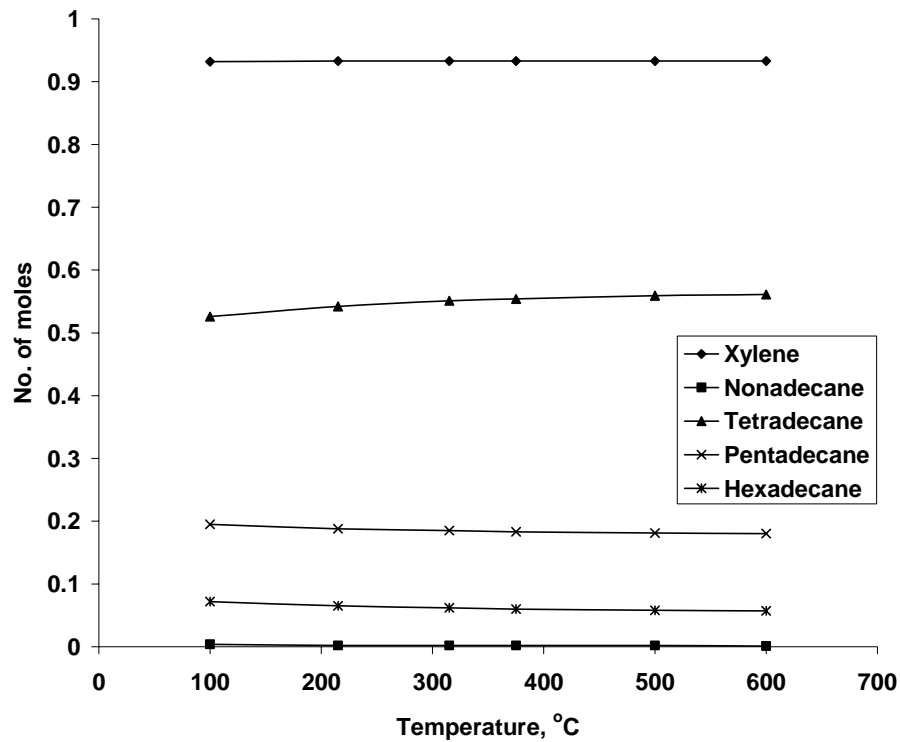


Figure 4.31 Thermodynamic analysis of Methyl Linoleate

smaller amount of hexadecane and nonadecane can be produced from one mole of methyl linoleate. Table 4.9 depicts the maximum amount of different hydrocarbons which can be produced from one mole of methyl linoleate.

Table 4.9 Number of moles of different hydrocarbons deoxygenated from one mole methyl linoleate at 375 °C

| <b>Compounds</b> | <b>Moles</b> |
|------------------|--------------|
| Xylene           | 0.933        |
| Tetradecane      | 0.554        |
| Pentadecane      | 0.183        |
| Hexadecane       | 0.060        |
| Nonadecane       | 0.002        |



## CHAPTER V

### SUMMARY AND CONCLUSIONS

#### 5.1 Summary

The base (potassium hydroxide) catalyzed transesterification of soybean oil using ultrasonic mixing produces acceptable yields of biodiesel (fatty acid methyl esters) in relatively short time. With the experiments conducted and collected data, some combination of time and amplitude can be recommended in UP400S (ultrasonic processor) for obtaining high yields of biodiesel. One can use 5 min/ 75 % amplitude, 5 min/ 100 % amplitude, 10 min/ 50 % amplitude or 15 min/ 25 % amplitude of UP400S for obtaining high yields of biodiesel with 100 cc of soybean oil, 25 cc methanol (6:1) and 1 g of potassium hydroxide. Analogously, we can provide an energy range of 1.4 to 2.41 kJ/g of soybean oil to obtain over 97% transesterification yield.

All the solid catalysts used in this study had somewhat different behavior towards transesterification reaction. Lead oxide catalysts were found to be good towards the transesterification and resulted in more than 89% of biodiesel yield. MgO and Pb<sub>3</sub>O<sub>4</sub> had shown an increasing trend from 75°C to 225°C which warrants higher temperature studies. Other than these two catalyst, all other tested catalysts displayed a trend towards cracking at higher temperatures. Tl<sub>2</sub>O<sub>3</sub> and ZnO, in spite of their opposite leaching behavior, displayed a similar trend towards transesterification. This can be attributed to

their approximately similar surface area. CaO was selective towards transesterification at all the three temperatures tested.

Base catalyzed transesterification of soybean oil using solid catalysts produces biodiesel under high pressure and high temperature conditions. A maximum biodiesel yield of 85% was obtained by BaO in 14 minutes, whereas, PbO, MnO<sub>2</sub>, CaO and MgO gave maximum yields of 84, 80, 78 and 66% respectively at 215 °C.

Out of all heterogeneous catalysts tested, the mixed metal oxide catalyst showed the highest yield towards transesterification. More than 99% of FAME yield was observed with NaMO1. Rest of NaMO (i.e. NaMO2, 3, 4) also got good yield of biodiesel. All the prepared catalysts were basic in nature.

The overall reaction order of PbO, MnO<sub>2</sub>, BaO, CaO, MgO and NaMO was found to be 1, 1, 3, 1, 1 and 3, respectively. The highest rate constant was observed for NaMO1 which was 429, m<sup>6</sup> mole<sup>-2</sup> min<sup>-1</sup> m<sup>-2</sup> of the catalyst.

As far as biodiesel upgrading is concerned, we were able to detect some deoxygenated hydrocarbons from methyl linoleate. Mass spectrometry was able to detect xylene, tetradecane, pentadecane, hexadecane, nonadecane and some more hydrocarbons (with high probability of more than 90%). The approximate theoretical amounts of these compounds were determined by a thermodynamic analysis. Accordingly, with this analysis, we can say that HZSM-5 was able to break the methyl esters in to deoxygenated hydrocarbons.

## 5.2 Conclusions

Based on the present study we concluded the following facts.

- Ultrasound energy can be effectively used for fast transesterification reaction rates in comparison to conventional impeller fitted batch reaction systems.
- Basic solid catalysts including MgO, Pb<sub>3</sub>O<sub>4</sub>, and the mixed oxide (NaMO1) prepared in this study can be effectively used for the transesterification reaction in order to rectify the problem of separation.
- Biodiesel can be upgraded using HZSM-5 catalysts at higher temperatures in order to deoxygenate the fatty acid methyl esters into lower molecular weight hydrocarbons (xylene, tetradecane, pentadecane, hexadecane, nonadecane and some other).

## CHAPTER VI

### RECOMMENDATIONS

Based on the present study, we make the following recommendations:

- Ultrasonication proved to be highly effective for homogeneous catalyzed transesterification. Accordingly, the effectiveness of this technology for the transesterification of triglycerides with solid catalyst needs to be investigated. This technology has the potential to be as effective for heterogeneously catalyzed process since ultrasound simultaneously provides sufficient amount of energy as well as mixing power to circumvent mass transfer limitations as opposed to conventional mixing.
- In the mixed oxides study, Na impregnated along with La proved to be an effective transesterification catalyst. However, we still observed some leaching. This opens up new doors to look at other heavy metals like cerium (Ce), copper (Co), zinc (Zn), thallium (Th) to be coupled/doped and tested for effectiveness for the transesterification.
- In the methyl esters upgrading study, it was revealed that pure ZSM-5 was able to produce deoxygenated products from biodiesel. Metal doping in zeolites are known to enhance catalytic activity of zeolites in numerous reactions. In light of

this, the ability of metal doped ZSM-5 to for deoxygenation of fatty acid methyl esters needs to be further investigated.

## LITERATURES CITED

- Adams, C., J. F. Peters, M. C. Rand, B. J. Schroer, M. C. Ziemke. 1983. Investigation of soybean oil as a diesel fuel extender: Endurance tests. *Journal of American Oil Chemical Society* 60:1574-1579.
- Adhikari, S., and coauthors. 2007a. A thermodynamic analysis of hydrogen production by steam reforming of glycerol. *International Journal of Hydrogen Energy* 32(14):2875-2880.
- Adhikari, S., S. Fernando, and A. Haryanto. 2007b. A comparative thermodynamic and experimental analysis on hydrogen production by steam reforming of glycerin. *Energy & Fuels* 21(4):2306-2310.
- Anon. 1982. Filtered used frying fat powers diesel fleet. *Journal of American Oil Chemical Society* 59:780A-781A.
- Baker, E. G., D. C. Elliott. 1988. Research in thermochemical biomass conversion. *Applied Science*. 14:883-889.
- Bartholomew, D. 1981. Vegetable oil fuel. *Journal of American Oil Chemical Society* 58:286A-288A.
- Benitez, F. A. 2004. Effect of the use of ultrasonic waves on biodiesel production in alkaline transesterification of bleached tallow and vegetable oils: cavitation model. University of Puerto Rico, Mayaguez.
- Bird, R. B., W. E. Stewart, and E. N. Lightfoot. 2002. *Transport phenomena*, 2<sup>nd</sup> edition. John Wiley & Sons, Inc, New York.
- Calvin, M. 1985. Fuel oils from higher plants. *Annalytical Process Phytochemistry Society*. 26:147-160.
- Certinkaya, M.K. 2004. Optimization of Base-catalyzed reaction of used cooking oil. *Energy & Fuels* 18(6):1888-1895.
- Chang, C. C., W. W. Wan. 1947. China's motor fuels from tung oil. *Industrial Engineering Chemistry Research* 39:1543-1548.

- Colucci, J. A., E. E. Borrero, F. Alape, 2005. Biodiesel from an alkaline transesterification reaction of soybean oil using ultrasonic mixing. *Journal of American Oil Chemical Society* 82:525-530.
- Darnoko, D., M. C. 2000. Kinetics of palm oil transesterification in a batch reactor. *Journal of American Oil Chemists Society* 77:1263-1267.
- Dean, M., S. Yoder, E. J. Doskocil. 2006. Nanocrystalline Metal Oxide-Based Catalysts for Biodiesel Production from Soybean Oil. *Catalysis and Reaction Engineering* 39:1-10.
- Demirbas, A. 2003. Biodiesel fuels from vegetable oils via catalytic and non-catalytic supercritical alcohol transesterifications and other methods: a survey. *Energy Conversion and Management* 44(13):2093-2109.
- Denbigh, K. 1966. *The principles of chemical equilibrium*. Cambridge University Press, London.
- De Vedia, M. R. 1944. Vegetable oil as a diesel fuel. *Diesel Power* 22:1298.
- Ertl, G., H. Knozinger, J. Weitkamp. 2000. *Handbook of heterogeneous catalysis*.
- Fernandes, A. C., C. C. Romao. 2006. Silane/MoO<sub>2</sub>Cl<sub>2</sub> as an efficient system for the reduction of esters. *Journal of Molecular Catalysis A: Chemical* 253:96-98.
- Filip, V.Z, V. Smidrkal, 1992. *Jornal of Farm Corps Grass* 39:91.
- Fishtik, I., A. Alexander, R. Datta, and D. Geana. 2000. A thermodynamic analysis of hydrogen production by steam reforming of ethanol via response reactions. *International Journal of Hydrogen Energy* 25(1):31-45.
- Freedman, B., E. H. Pryde. 1986. Transesterification kinetics of soybean oil. *Journal of American Oil Chemists Society* 63(10):1375-1380.
- Freund, R. J., and W. J. Wilson. 1997. *Statistical methods*. Academic Press, San Diego.
- García, E. Y., and M. A. Laborde. 1991. Hydrogen production by the steam reforming of ethanol: thermodynamic analysis. *International Journal of Hydrogen Energy* 16(5):307-312.
- Gol'dberg, K. M., M. M. Fal'kovich, I. A. Zarskii. 1966. Continuous alcholysis of vegetable oils with sonic vibrations. *Journal written in Russian*. 2:63-67.
- Grossley, T. D., T. D. Heyes, B. J. F. Hudson. 1962. The effect of heat on pure triglycerides. *Journal of American Oil Chemical Society* 39:9-14.

- Gryglewicz, S. 1999. Rapeseed oil methyl esters preparation using heterogeneous catalysts. *Bioresource Technology* 70:249-253.
- Kubickova, I., M. Snare, K. Eranen, P. M. Arvela, D. Y. Murzin. 2005. Hydrocarbons for diesel fuel via decarboxylation of vegetable oils. *Catalysis Today* 106:197-200.
- Li, Z. 2005. Novel solid base catalysts for Michael additions synthesis, characterization and application. Thesis. Germany
- Lide, D. R. 2005-2006. CRC handbook of chemistry and physics, 86th edition. CRC Press, Florida.
- Liu, X., H. He, Y. Wang, S. Zhu. 2007. Transesterification of soybean oil to biodiesel using SrO as a solid base catalyst. *Catalysis Communications* 8(7):1107-1111.
- Lowell, S., J. E. Shields, M. A. Thomas, and M. Thommes. 2006. Characterization of porous solids and powders: surface area, pore size and density. Springer, Dordrecht, The Netherlands.
- Lwin, Y., W. R. W. Daud, A. B. Mohamad, and Z. Yaakob. 2000. Hydrogen production from steam-methanol reforming: thermodynamic analysis. *International Journal of Hydrogen Energy* 25(1):47-53.
- Ma, F., M. A. Hanna. 1999. Biodiesel Production: A review. *Bioresource Technology* 70:1-15.
- Maggi, R., B. Delmon. 1995. *Coal Science Technology* 24:885.
- Nagel, N., P. Lemke. 1990. Production of methyl fuel from Microalgae: Application *Biochemistry Biotechnology*. 24:355-361.
- Niehaus, R.A., C. E. Goering, L. D. Savage, S. C. Sorenson. 1986. Cracked soybean oil as a fuel for a diesel engine. *Transactions of ASAE* 29:683-689.
- Noureddini, H., D. Z. 1997. Kinetics of transesterification of soybean oil. *Journal of American Oil Chemists Society* 74:1457-1463.
- Peterson, C. L. 1986. Vegetable oil as a diesel fuel: Status and research priorities. *Transactions of ASAE* 29(5):1413.
- Perry, R. H., D. W. Green, and J. O. Maloney. 1997. Perry's chemical engineer's handbook, seventh edition. McGraw-Hill, New York.
- Pioch, D., P. Lozano, M. C. Rasoanantoandro, J. Graille, P. Geneste, A. Guida. 1993. Biofuels from catalytic cracking of tropical vegetable oils. *Oleagineux* 48:289-291.



- Pryde, E. H. 1983. Vegetable oil as a diesel fuel: Overview. *Journal of American Oil Chemical Society* 60:1557-1558.
- Rase, H. F. 1977. *Chemical reactor design for process plants: principles and techniques*. John Wiley & Sons, New York.
- Schlick, M. L., M. A. Hanna, J. L. Schinstock. 1988. Soybean and sunflower oil performance in a diesel engine. *Transactions of ASAE* 31(5):1345-1349.
- Schuchardt, U., R. Sercheli, M. R. Vargas. 1998. Transesterification of vegetable oils: A review. *Journal of Brazilian Chemical Society* 9(1):199-210.
- Schwab, A.W., G. J. Dykstra, E. Selke, S. C. Sorenson, E. H. Pryde. 1988. Diesel fuel from thermal decomposition of soybean oil. *Journal of American Oil Chemical Society* 65:1781-1786.
- Semelsberger, T. A., and R. L. Borup. 2006. Thermodynamic equilibrium calculations of hydrogen production from the combined processes of dimethyl ether steam reforming and partial oxidation. *Journal of Power Sources* 155:340-352.
- Senol, O. I., T. R. Viljava, A. O. I. Krause. 2005. Hydrodeoxygenation of methyl esters on sulphided NiMo/g-Al<sub>2</sub>O<sub>3</sub> and CoMo/g-Al<sub>2</sub>O<sub>3</sub> catalysts. *Catalysis Today* 100:331-335.
- Serio, M. D., M. Ledda, M. Cozzolino, G. Minutillo, R. Tesser, E. Santacesaria. 2006. Transesterification of Soybean Oil to Biodiesel by Using Heterogeneous Basic Catalysts. *Industrial Engineering Chemistry Research* 45:3009-3014.
- Shah, S., A. Sharma, M. N. Gupta. 2005. Extraction of oil from *Jatropha curcas L.* seed kernels by combination of ultrasonication and aqueous enzymatic oil extraction. *Bioresource Technology* 96:121-123.
- Shay, E. G. 1993. Diesel fuel from vegetable oils: status and opportunities. *Biomass and Bioenergy* 4:227-242.
- Sheu, Y. H. E., R. G. Anthony, E. J. Soltes. 1988. *Fuel Processing Technology* 19:31.
- Shumaker, J. L, C. Crofcheck, S. A. Tackett, E. S. Jimenez, M. Crocker. 2007. Biodiesel production from soybean oil using calcined Li–Al layered double hydroxide catalysts. *Catalysis Letters* 115(1-2):56-61.
- Singh, A. K., S. D. Fernando. 2007. Reaction Kinetics of Soybean Oil Transesterification Using heterogeneous Metal Oxide Catalysts. *Chemical Engineering Technology* 30(12):1-6.

- Sipila, K., E. Kuoppala, L. Fagernas, A. Oasmaa. 1988. *Biomass Bioenergy* 14:103.
- Smith, W. R., and R. W. Missen. 1982. *Chemical reaction equilibrium analysis: theory and algorithms*. John Wiley & Sons, New York.
- Stavarache, C., M. Vinatoru, R. Nishimura, Y. Maeda. 2003. Conversion of vegetable oil to biodiesel using ultrasonic irradiation. *Chemistry Letters* 32(8):716-717.
- Stavarache, C., M. Vinatoru, R. Nishimura, Y. Maeda. 2005. Fatty acids methyl esters from vegetable oils by means of ultrasonic energy. *Ultrasonic Sonochemistry* 12:367-372.
- Suppes, G. J., M.A.D., E. J. Doskocil, P. J. Mankidy, M. J. Goff. 2004. *Applied Catalysis, A: General* 257:213-223.
- Twigg, M. V. 1989. *Catalyst handbook*, second edition. Wolfe Publishing Ltd, Frome, England.
- Ultrasonic laboratory devices (manual). Hielscher: Ringwood, NJ; [www.hielscher.com](http://www.hielscher.com).
- Vasudeva, K., N. Mitra, P. Umasankar, and S. C. Dhingra. 1996. Steam reforming of ethanol for hydrogen production: thermodynamic analysis. *International Journal of Hydrogen Energy* 21(1):13-18.
- Vitolo, S., M. Seggiani, P. Frediani, G. Ambrosini, L. Politi. 1999. Catalytic upgrading of pyrolytic oils to fuel over different zeolites. *Fuel* 78:1147-1159.
- Vitolo, S., B. Bresci, M. Seggiani, M. G. Gallo. 2001. Catalytic upgrading of pyrolytic oils over HZSM-5 zeolite: behaviour of the catalyst when used in repeated upgrading-regenerating cycles. *Fuel* 80:17-26.
- Wang, G., S. Yan, C. Zhou, B. Liang. 2005. Preparation and activity measurement of CaO/ MgO catalyst for biodiesel fuel production. *Zhongguo Youzhi (Journal Written in Chinese)* 30(10):66-69.
- Wen, Z. Y., Z. X. Lin, K. G. Chen. 1996. Introduction of sodium to layered double hydroxides  $\text{LiAl}_2(\text{OH})_7 \cdot 2\text{H}_2\text{O}$ . *Journal of Materials Science Letters* 15:105-106.
- Wu, H., M. Zong. 2005. Effect of ultrasonic irradiation on enzymatic transesterification of waste oil to biodiesel. *Fuel Chemistry* 50(2): 773-774.
- Xie, W.P., Hong, Chen, Ligong. 2006. *Applied Catalysis, A:General* 300(1):67-74.
- Yaws, C. L. 1999. *Chemical properties handbook*. McGraw Hill, New York.

- Zhu, J., Y. Chun, Y. Wang, Q. Xu. 1999. Attempts to create new shape –selective solid strong base catalysts. *Catalysis Today* 51:103-111.
- Zhu, H., Z. Wu, Y. Chen, P. Zhang, S. Duan, X. Liu, Z. Mao. 2006. Preparation of Biodiesel Catalyzed by Solid Super Base of Calcium Oxide and Its Refining Process. *Chinese Journal of Catalysis* 27(5):391-396.
- Ziejewski, M., K. R. Kaufman, A. W. Schwab, E. H. Pryde. 1984. Diesel engine evaluation of a nonionic sunflower oil-aqueous ethanol microemulsions. *Journal of American Oil Chemical Society* 61:1620-1626.

## APPENDIX A

### KINETICS DATA FOR ALL THE SOLID CATALYSTS

## APPENDIX – A

Appendix – A presents the kinetic data for all the selected catalysts.

### MgO

| Time,min | FAME, % | Conversion, X | $C_0^{TG}$ | $C_0^{ME}$ | $C^{TG}$ | $C^{ME}$ |
|----------|---------|---------------|------------|------------|----------|----------|
| 0        | 3.348   | 0.03348       | 0.1        | 0.6        | 0.096652 | 0.589956 |
| 15       | 1.954   | 0.01954       | 0.1        | 0.6        | 0.098046 | 0.594138 |
| 30       | 4.949   | 0.04949       | 0.1        | 0.6        | 0.095051 | 0.585153 |
| 45       | 14.121  | 0.14121       | 0.1        | 0.6        | 0.085879 | 0.557637 |
| 60       | 31.189  | 0.31189       | 0.1        | 0.6        | 0.068811 | 0.506433 |
| 75       | 44.4    | 0.444         | 0.1        | 0.6        | 0.0556   | 0.4668   |
| 90       | 52.725  | 0.52725       | 0.1        | 0.6        | 0.047275 | 0.441825 |
| 105      | 58.451  | 0.58451       | 0.1        | 0.6        | 0.041549 | 0.424647 |
| 120      | 66.765  | 0.66765       | 0.1        | 0.6        | 0.033235 | 0.399705 |

### PbO

| Time,min | FAME, % | Conversion, X | $C_0^{TG}$ | $C_0^{ME}$ | $C^{TG}$ | $C^{ME}$ |
|----------|---------|---------------|------------|------------|----------|----------|
| 0        | 4.383   | 0.04383       | 0.1        | 0.6        | 0.095617 | 0.586851 |
| 15       | 4.513   | 0.04513       | 0.1        | 0.6        | 0.095487 | 0.586461 |
| 30       | 50.428  | 0.50428       | 0.1        | 0.6        | 0.049572 | 0.448716 |
| 45       | 81.583  | 0.81583       | 0.1        | 0.6        | 0.018417 | 0.355251 |
| 60       | 84.529  | 0.84529       | 0.1        | 0.6        | 0.015471 | 0.346413 |

### MnO<sub>2</sub>

| Time,min | FAME, % | Conversion, X | $C_0^{TG}$ | $C_0^{ME}$ | $C^{TG}$ | $C^{ME}$ |
|----------|---------|---------------|------------|------------|----------|----------|
| 0        | 0.776   | 0.00776       | 0.1        | 0.6        | 0.099224 | 0.597672 |
| 15       | 2.191   | 0.02191       | 0.1        | 0.6        | 0.097809 | 0.593427 |
| 30       | 2.264   | 0.02264       | 0.1        | 0.6        | 0.097736 | 0.593208 |
| 45       | 5.183   | 0.05183       | 0.1        | 0.6        | 0.094817 | 0.584451 |
| 60       | 39.9    | 0.399         | 0.1        | 0.6        | 0.0601   | 0.4803   |
| 75       | 57.646  | 0.57646       | 0.1        | 0.6        | 0.042354 | 0.427062 |
| 90       | 71.446  | 0.71446       | 0.1        | 0.6        | 0.028554 | 0.385662 |
| 105      | 77.856  | 0.77856       | 0.1        | 0.6        | 0.022144 | 0.366432 |
| 120      | 80.54   | 0.8054        | 0.1        | 0.6        | 0.01946  | 0.35838  |

**BaO**

| Time,min | FAME, % | Conversion, X | $C^{TG}_0$ | $C^{ME}_0$ | $C^{TG}$ | $C^{ME}$ |
|----------|---------|---------------|------------|------------|----------|----------|
| 0        | 64.624  | 0.64624       | 0.1        | 0.6        | 0.035376 | 0.406128 |
| 2        | 81.96   | 0.8196        | 0.1        | 0.6        | 0.01804  | 0.35412  |
| 4        | 82.25   | 0.8225        | 0.1        | 0.6        | 0.01775  | 0.35325  |
| 6        | 84.35   | 0.8435        | 0.1        | 0.6        | 0.01565  | 0.34695  |
| 8        | 84.73   | 0.8473        | 0.1        | 0.6        | 0.01527  | 0.34581  |

**CaO**

| Time,min | FAME, % | Conversion, X | $C^{TG}_0$ | $C^{ME}_0$ | $C^{TG}$ | $C^{ME}$ |
|----------|---------|---------------|------------|------------|----------|----------|
| 0        | 71.42   | 0.7142        | 0.1        | 0.6        | 0.02858  | 0.38574  |
| 2        | 78.07   | 0.7807        | 0.1        | 0.6        | 0.02193  | 0.36579  |
| 4        | 76.7    | 0.767         | 0.1        | 0.6        | 0.0233   | 0.3699   |

**NaMO1 at 100°C**

| Time,min | FAME, % | Conversion, X | $C^{TG}_0$ | $C^{ME}_0$ | $C^{TG}$ | $C^{ME}$ |
|----------|---------|---------------|------------|------------|----------|----------|
| 0        | 0       | 0             | 0.0008     | 0.0048     | 0.0008   | 0.0048   |
| 30       | 8.01    | 0.0801        | 0.0008     | 0.0048     | 0.000736 | 0.004608 |
| 60       | 18.93   | 0.1893        | 0.0008     | 0.0048     | 0.000649 | 0.004346 |
| 90       | 31.5    | 0.315         | 0.0008     | 0.0048     | 0.000548 | 0.004044 |

**NaMO1 at 215°C**

| Time,min | FAME, % | Conversion, X | $C^{TG}_0$ | $C^{ME}_0$ | $C^{TG}$ | $C^{ME}$ |
|----------|---------|---------------|------------|------------|----------|----------|
| 0        | 0       | 0             | 0.0008     | 0.0048     | 0.0008   | 0.0048   |
| 30       | 91.62   | 0.9162        | 0.0008     | 0.0048     | 6.7E-05  | 0.002601 |
| 60       | 94.46   | 0.9446        | 0.0008     | 0.0048     | 4.43E-05 | 0.002533 |
| 90       | 98.3    | 0.983         | 0.0008     | 0.0048     | 1.36E-05 | 0.002441 |
| 120      | 99.3    | 0.993         | 0.0008     | 0.0048     | 5.6E-06  | 0.002417 |

Where,

X is the conversion

$C^{TG}_0$  and  $C^{ME}_0$  are the initial concentration of triglyceride and methanol respectively.

$C^{TG}$  and  $C^{ME}$  are the final concentration of triglyceride and methanol respectively.

## APPENDIX B

### DATA FOR THERMODYNAMIC ANALYSIS OF METHYL LINOLEATE

## APPENDIX – B

Appendix – B depicts the data for the thermodynamic analysis of methyl linoleate.

The first part of Appendix – B shows all the Gibbs energy data for different deoxygenated product at different temperatures of 100, 215, 315, 375, 500 and 600 °C.

### 100 °C

| Species     | A        | B       | C        | G        | R        | G/RT     |
|-------------|----------|---------|----------|----------|----------|----------|
| Xylene      | 15.063   | 0.33452 | 4.14E-05 | 1.46E+02 | 0.008314 | 46.94981 |
| Nonadecane  | -444.994 | 1.815   | 1.29E-04 | 2.50E+02 | 0.008314 | 80.58462 |
| Tetradecane | -339.495 | 1.33    | 9.84E-05 | 1.70E+02 | 0.008314 | 54.91042 |
| Pentadecane | -360.562 | 1.4269  | 1.05E-04 | 1.86E+02 | 0.008314 | 60.04982 |
| Hexadecane  | -381.687 | 1.5241  | 1.10E-04 | 2.02E+02 | 0.008314 | 65.19269 |

### 215 °C

| Species     | A        | B       | C        | G        | R        | G/RT     |
|-------------|----------|---------|----------|----------|----------|----------|
| Xylene      | 15.063   | 0.33452 | 4.14E-05 | 1.88E+02 | 0.008314 | 46.37764 |
| Nonadecane  | -444.994 | 1.815   | 1.29E-04 | 4.71E+02 | 0.008314 | 116.1797 |
| Tetradecane | -339.495 | 1.33    | 9.84E-05 | 3.33E+02 | 0.008314 | 82.06974 |
| Pentadecane | -360.562 | 1.4269  | 1.05E-04 | 3.61E+02 | 0.008314 | 88.89566 |
| Hexadecane  | -381.687 | 1.5241  | 1.10E-04 | 3.88E+02 | 0.008314 | 95.72516 |

### 315 °C

| Species     | A        | B       | C        | G        | R        | G/RT     |
|-------------|----------|---------|----------|----------|----------|----------|
| Xylene      | 15.063   | 0.33452 | 4.14E-05 | 2.26E+02 | 0.008314 | 46.24403 |
| Nonadecane  | -444.994 | 1.815   | 1.29E-04 | 6.67E+02 | 0.008314 | 136.3803 |
| Tetradecane | -339.495 | 1.33    | 9.84E-05 | 4.77E+02 | 0.008314 | 97.48387 |
| Pentadecane | -360.562 | 1.4269  | 1.05E-04 | 5.15E+02 | 0.008314 | 105.2673 |
| Hexadecane  | -381.687 | 1.5241  | 1.10E-04 | 5.53E+02 | 0.008314 | 113.053  |

### 375 °C

| Species     | A        | B       | C        | G        | R        | G/RT     |
|-------------|----------|---------|----------|----------|----------|----------|
| Xylene      | 15.063   | 0.33452 | 4.14E-05 | 2.49E+02 | 0.008314 | 46.25741 |
| Nonadecane  | -444.994 | 1.815   | 1.29E-04 | 7.85E+02 | 0.008314 | 145.7372 |
| Tetradecane | -339.495 | 1.33    | 9.84E-05 | 5.64E+02 | 0.008314 | 104.6241 |
| Pentadecane | -360.562 | 1.4269  | 1.05E-04 | 6.08E+02 | 0.008314 | 112.8512 |
| Hexadecane  | -381.687 | 1.5241  | 1.10E-04 | 6.52E+02 | 0.008314 | 121.0795 |



**500 °C**

| <b>Species</b> | <b>A</b> | <b>B</b> | <b>C</b> | <b>G</b> | <b>R</b> | <b>G/RT</b> |
|----------------|----------|----------|----------|----------|----------|-------------|
| Xylene         | 15.063   | 0.33452  | 4.14E-05 | 2.98E+02 | 0.008314 | 46.42754    |
| Nonadecane     | -444.994 | 1.815    | 1.29E-04 | 1.03E+03 | 0.008314 | 161.0284    |
| Tetradecane    | -339.495 | 1.33     | 9.84E-05 | 7.47E+02 | 0.008314 | 116.2935    |
| Pentadecane    | -360.562 | 1.4269   | 1.05E-04 | 8.05E+02 | 0.008314 | 125.246     |
| Hexadecane     | -381.687 | 1.5241   | 1.10E-04 | 8.62E+02 | 0.008314 | 134.1968    |

**600 °C**

| <b>Species</b> | <b>A</b> | <b>B</b> | <b>C</b> | <b>G</b> | <b>R</b> | <b>G/RT</b> |
|----------------|----------|----------|----------|----------|----------|-------------|
| Xylene         | 15.063   | 0.33452  | 4.14E-05 | 3.39E+02 | 0.008314 | 46.65686    |
| Nonadecane     | -444.994 | 1.815    | 1.29E-04 | 1.24E+03 | 0.008314 | 170.5075    |
| Tetradecane    | -339.495 | 1.33     | 9.84E-05 | 8.97E+02 | 0.008314 | 123.5279    |
| Pentadecane    | -360.562 | 1.4269   | 1.05E-04 | 9.65E+02 | 0.008314 | 132.9304    |
| Hexadecane     | -381.687 | 1.5241   | 1.10E-04 | 1.03E+03 | 0.008314 | 142.3284    |

Where,

A, B, C are coefficient of Gibbs free energy

G is the Gibbs free energy

R is Gas constant

T is the absolute temperature.

Formation of different compounds (number of moles) after deoxygenation of methyl linoleate at different temperature is shown in the following table.

| <b>Species</b> | <b>100 °C</b> | <b>215 °C</b> | <b>315 °C</b> | <b>375 °C</b> | <b>500 °C</b> | <b>600 °C</b> |
|----------------|---------------|---------------|---------------|---------------|---------------|---------------|
| Xylene         | 0.932         | 0.933         | 0.933         | 0.933         | 0.933         | 0.933         |
| Nonadecane     | 0.0038        | 0.002         | 0.002         | 0.002         | 0.002         | 0.001         |
| Tetradecane    | 0.526         | 0.542         | 0.551         | 0.554         | 0.559         | 0.561         |
| Pentadecane    | 0.195         | 0.188         | 0.185         | 0.183         | 0.181         | 0.18          |
| Hexadecane     | 0.072         | 0.065         | 0.062         | 0.06          | 0.058         | 0.057         |

Second part of the Appendix- B gives the coding with SAS 9.2 for thermodynamic analysis at all temperatures.

### At 100 °C

```
proc nlp tech=tr pall;
  array c[5] 46.94981104 80.58461693 54.91041704 60.04981772 65.19269134;
  array x[5] x1-x5;
  min y;
  parms x1-x5 = .1;
  bounds 1.e-6 <= x1-x5;
  lincon 19. = 8. * x1 + 19. * x2 + 14. *x3 + 15. *x4 + 16. *x5,
         34. = 10. * x1 + 40. * x2 + 30. *x3 + 32. * x4 + 34 *x5,
         2. = 0;

  s = x1 + x2 + x3 + x4 + x5;
  y = 0.;
  do j = 1 to 5;
    y = y + x[j] * (c[j] + log(x[j] / s));
  end;
run;
```

### At 215 °C

```
proc nlp tech=tr pall;
  array c[5] 46.37763523 116.179698 82.06974315 88.89565584 95.72516096 ;
  array x[5] x1-x5;
  min y;
  parms x1-x5 = .1;
  bounds 1.e-6 <= x1-x5;
  lincon 19. = 8. * x1 + 19. * x2 + 14. *x3 + 15. *x4 + 16. *x5,
         34. = 10. * x1 + 40. * x2 + 30. *x3 + 32. * x4 + 34 *x5,
```

```

                2. = 0;

s = x1 + x2 + x3 + x4 + x5;
y = 0.;
do j = 1 to 5;
    y = y + x[j] * (c[j] + log(x[j] / s));
end;
run;

```

### At 315 °C

```

proc nlp tech=tr pall;
    array c[5] 46.24403451 136.3802554 97.48386709 105.2673033 113.0530345 ;
    array x[5] x1-x5;
    min y;
    parms x1-x5 = .1;
    bounds 1.e-6 <= x1-x5;
    lincon 19. = 8. * x1 + 19. * x2 + 14. *x3 + 15. *x4 + 16. *x5,
           34. = 10. * x1 + 40. * x2 + 30. *x3 + 32. * x4 + 34 *x5,
           2. = 0;

s = x1 + x2 + x3 + x4 + x5;
y = 0.;
do j = 1 to 5;
    y = y + x[j] * (c[j] + log(x[j] / s));
end;
run;

```

### At 375 °C

```

proc nlp tech=tr pall;
    array c[5] 46.25741477 145.7371932 104.6240898 112.8512149 121.0794963 ;

```

```

array x[5] x1-x5;
min y;
parms x1-x5 = .1;
bounds 1.e-6 <= x1-x5;
lincon 19. = 8. * x1 + 19. * x2 + 14. *x3 + 15. *x4 + 16. *x5,
       34. = 10. * x1 + 40. * x2 + 30. *x3 + 32. * x4 + 34 *x5,
       2. = 0;

s = x1 + x2 + x3 + x4 + x5;
y = 0.;
do j = 1 to 5;
  y = y + x[j] * (c[j] + log(x[j] / s));
end;
run;

```

### **At 500 °C**

```

Proc nlp tech=tr pall;
array c[5] 46.42754 161.028446 116.2934819 125.2460092 134.196773 ;
array x[5] x1-x5;
min y;
parms x1-x5 = .1;
bounds 1.e-6 <= x1-x5;
lincon 19. = 8. * x1 + 19. * x2 + 14. *x3 + 15. *x4 + 16. *x5,
       34. = 10. * x1 + 40. * x2 + 30. *x3 + 32. * x4 + 34 *x5,
       2. = 0;

s = x1 + x2 + x3 + x4 + x5;
y = 0.;
do j = 1 to 5;
  y = y + x[j] * (c[j] + log(x[j] / s));
end;
run;

```

### **At 600 °C**

```

proc nlp tech=tr pall;
array c[5] 46.6568615 170.5074864 123.5279418 132.9304124 142.3284245 ;

```

```

array x[5] x1-x5;
min y;
parms x1-x5 = .1;
bounds 1.e-6 <= x1-x5;
lincon 19. = 8. * x1 + 19. * x2 + 14. *x3 + 15. *x4 + 16. *x5,
       34. = 10. * x1 + 40. * x2 + 30. *x3 + 32. * x4 + 34 *x5,
       2. = 0;
s = x1 + x2 + x3 + x4 + x5;
y = 0.;
do j = 1 to 5;
  y = y + x[j] * (c[j] + log(x[j] / s));
end;
run;

```